

Discovery of Novel and Potent Thiazoloquinazolines as Selective Aurora A and B Kinase Inhibitors

Frédéric H. Jung,^{*,†} Georges Pasquet,[‡] Christine Lambert-van der Brempt,[‡] Jean-Jacques M. Lohmann,[‡] Nicolas Warin,[‡] Fabrice Renaud,[‡] Hervé Germain,[‡] Chris De Savi,[‡] Nicola Roberts,[‡] Trevor Johnson,[‡] Cyril Dousson,[‡] George B. Hill,[‡] Andrew A. Mortlock,[‡] Nicola Heron,[‡] Robert W. Wilkinson,[‡] Stephen R. Wedge,[‡] Simon P. Heaton,[‡] Rajesh Odedra,[‡] Nicholas J. Keen,[‡] Stephen Green,[‡] Elaine Brown,[‡] Katherine Thompson,[‡] and Stephen Brightwell[‡]

AstraZeneca, Centre de Recherches, Parc Industriel Pompelle, BP1050, Chemin de Vrilly, 51689 Reims Cedex2, France, and AstraZeneca, Alderley Park, Macclesfield, Cheshire SK10 4TG, United Kingdom

Received August 10, 2005

The synthesis of a novel series of quinazolines substituted at C4 by five-membered ring aminoheterocycles is reported. Their in vitro structure–activity relationships versus Aurora A and B serine-threonine kinases is discussed. Our results demonstrate that quinazolines with a substituted aminothiazole at C4 possess potent Aurora A and B inhibitory activity and excellent selectivity against a panel of various serine-threonine and tyrosine kinases, as exemplified by compound **46**. We found also that the position and nature of the substituent on the thiazole play key roles in cellular potency. Compounds with an acetanilide substituent at C5' have the greatest cellular activity. The importance of the C5' position for substitution has been rationalized by ab initio molecular orbital calculations. Results show that the planar conformation with the sulfur of the thiazole next to the quinazoline N-3 is strongly favored over the other possible planar conformation. Compound **46** is a potent suppressor of the expression of phospho-histone H3 in tumor cells in vitro as well as in vivo, where **46**, administered as its phosphate prodrug **54**, suppresses the expression of phospho-histone H3 in subcutaneously implanted tumors in nude mice.

Introduction

Mammals express three Aurora kinase paralogues, Aurora A, B, and C,¹ each of which is thought to play important roles in regulating mitosis. The Aurora kinases are expressed at low levels in most tissues but are highly expressed in mitotically active cells such as thymus, testis, spleen, intestine, and bone marrow.^{1,2} Indeed, the expression and kinase activity of Aurora A and B are cell cycle regulated; they are only expressed during mitosis and are only active as kinases during mitosis. Interestingly, Aurora A and B display strikingly distinct subcellular localizations during mitosis. Aurora A localizes to the centrosomes and the mitotic spindle from prophase to telophase,^{2,3} while Aurora B is a chromosomal passenger protein that localizes to the kinetochores of chromosomes in the prophase and metaphase and subsequently to the spindle midzone during anaphase and to the postmitotic bridge of telophase cells. Determining the functions of the Aurora kinases is currently an active area of research, and as the findings are extensively reviewed elsewhere,⁴ the biological roles of each protein will be only briefly discussed.

Aurora B is implicated in chromosomal alignment and separation;^{5,6} it has also been shown to play a role in the tension sensing machinery of the spindle checkpoint,⁷ as well as targeting checkpoint proteins to kinetochores in anaphase onset⁸ and cytokinesis.⁹ Aurora B also interacts with a number of chromosomal passenger proteins, including the inner centromere protein (INCENP) to facilitate proper chromosomal biorientation and segregation.^{9–11} It has recently been shown that the interaction of Aurora B with survivin helps to target this kinase to its substrates.^{12–15}

Aurora A is thought to play many roles in mitosis, and overexpression of Aurora A in mammalian cells leads to centrosome amplification and polyploidy.^{2,16} Overexpression of Aurora A has also been shown to override the checkpoint mechanism that monitors spindle assembly, allowing anaphase to occur despite continued activation of the spindle checkpoint.^{17,18} Finally, Aurora B is known to phosphorylate histone H3 during mitosis, which may play a role in chromosome condensation.^{19–21}

These findings suggest that overexpression of the Aurora kinases may be an important factor in chromosomal instability and is thus of potential importance in cancer. In support of this, Aurora A and B are frequently overexpressed in many cancer cells, offering strong evidence for a causal role in tumor progression.^{1–3,22,23} This has led to the suggestion that inhibiting the kinase activity of Aurora A and B may have therapeutic utility in cancer. A number of compounds belonging to various structural families have been reported to possess inhibitory activity against Aurora A and B with sufficient selectivity for Aurora kinases to allow the phenotype resulting from inhibition of these enzymes to be explored both in vitro and in vivo.^{8,24,25,55}

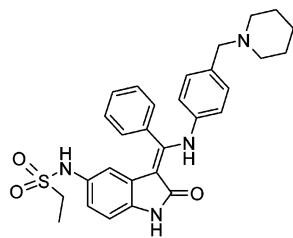
The chemical tools that have been most widely used are hesperadin, VX-680, and ZM447439. Hesperadin is a novel indolinone that inhibits Aurora B with an IC₅₀ value of 0.25 μmol when assayed against Aurora B immunoprecipitated from mitotic cells.²⁵ Hesperadin appears more potent in cell-based assays, with 0.02–0.1 μmol being sufficient to reduce mitotic histone H3 phosphorylation and presumably to effectively suppress Aurora B kinase activity. ZM447439, a quinazoline derivative, is an ATP-competitive inhibitor that, in in vitro kinase assays, inhibits Aurora A and B kinases with IC₅₀ values of approximately 0.1 μmol.⁸ This inhibition is relatively specific, with ZM447439 showing no inhibition (IC₅₀ > 10 μmol) of a range of kinases including CDK1 and PLK1. Most recently published is VX-680, which is a 4,6-diaminopyrimidine that

* To whom correspondence should be addressed. Tel: 33 3 26 61 68 47. Fax: 33 3 26 61 68 42. E-mail: Frederic.Jung@astrazeneca.com.

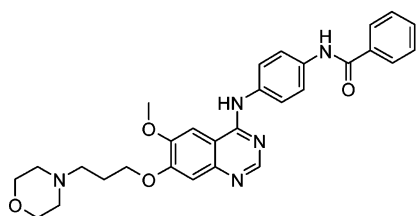
[†] AstraZeneca, Reims, France

[‡] AstraZeneca, Alderley Park, UK.

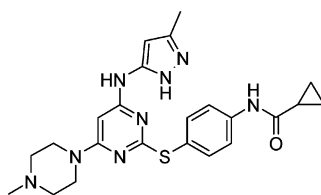
inhibits Aurora A, B, and C *in vitro* with inhibition constants of 0.0006, 0.018, and 0.0046 μmol , respectively, but does not appear to inhibit the majority of other kinases tested with the exception of the *fms*-related tyrosine kinase 3 (FLT-3), which is inhibited with a K_i of 0.030 μmol .²⁴



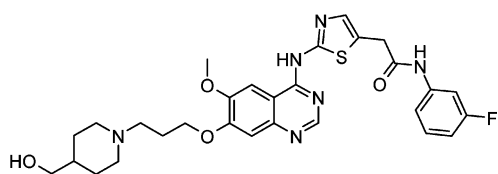
Hesperadin



ZM447439



VX-680



46

None of the inhibitors described to date are specific for the different paralogues and are likely to inhibit Aurora A, B, and C in cells. These three novel inhibitors all induce similar phenotypic changes when used in cell-based assays^{8,24,25} that most closely resemble those described for inhibition of Aurora B rather than Aurora A. All three compounds inhibit phosphorylation of histone H3 on serine 10 and inhibit cytokinesis. However, the cells do not undergo a simple mitotic arrest, the cell cycle proceeds with normal timing, and entry and exit from mitosis are unaffected.^{8,25} This cell cycle progression without resulting cytokinesis induces tetraploid cells. Longer exposures reveal cell-line-dependent effects. Treated cells either continue to cycle without cytokinesis and become highly polyploid (and ultimately die) or alternatively undergo a G1-like cell cycle arrest.⁸

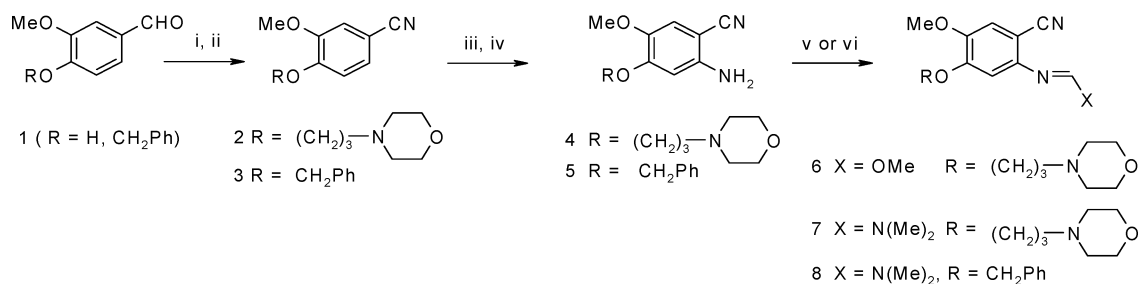
Encouragingly VX-680 displays potent antitumor activity in rodent tumor xenograft models, is well-tolerated preclinically, and has subsequently entered clinical development. These findings make it highly desirable to identify additional small

molecule inhibitors of Aurora kinases with improved properties and potency to evaluate their utility in the treatment of human cancers.

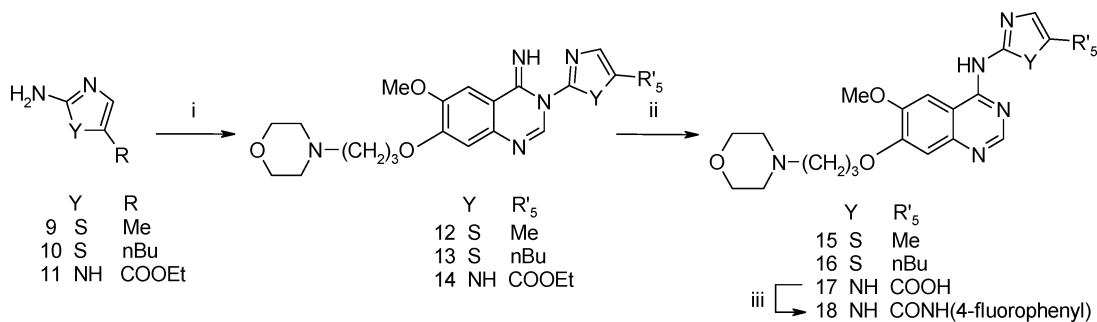
ZM447439 demonstrated good activity against the Aurora kinases, shows reasonable cellular potency, and is selective versus a range of other kinases, making it an attractive tool to probe further the mechanism and cellular phenotype of an Aurora kinase inhibitor.⁸ However, despite the utility of ZM447439 as a tool for exploring Aurora kinase function, it has relatively low aqueous solubility (10 μmol in pH 7.4 phosphate buffer) and is also highly protein bound (0.3% free drug in rat plasma). In this paper, we report the design, synthesis, and *in vitro* structure–activity relationships (SAR) of a novel, highly potent, and selective series of thiazoloquinazolines. This work ultimately led to compound **46**, which shows excellent activity in cells consistent with the inhibition of Aurora kinases and good physicochemical and pharmacokinetic properties and possesses potent *in vivo* activity in pharmacodynamic models.

Design of Substituted Quinazolines as Aurora Kinase Inhibitors. Knowledge from other quinazoline-based kinase inhibitors, such as Iressa, suggested that the ZM447439 should bind into the adenine site (with N-1 making a critical interaction with the protein backbone) and indicated that the extended benzamido group should occupy the selectivity pocket, thus playing an important role in its activity and selectivity. It was envisaged that further improvements in terms of both potency and physical properties could be made by substituting the benzamido phenyl ring and also by introducing more hydrophilic substituents onto the quinazoline ring. Four related pieces of medicinal chemistry were undertaken: (a) examination of five-membered ring amino-heterocyclic replacements in place of the aniline group in ZM447439 to reduce lipophilicity and to study the effect of ring replacement on potency and selectivity, (b) replacement of the amide linker group with the objective to optimize the binding of our inhibitors; (c) investigation of the impact of substitution in the benzamido ring, and (d) investigation of various quinazoline C7 substituents on physicochemical properties and potency. In all cases, we studied the *in vitro* cellular effect of Aurora kinase inhibition.

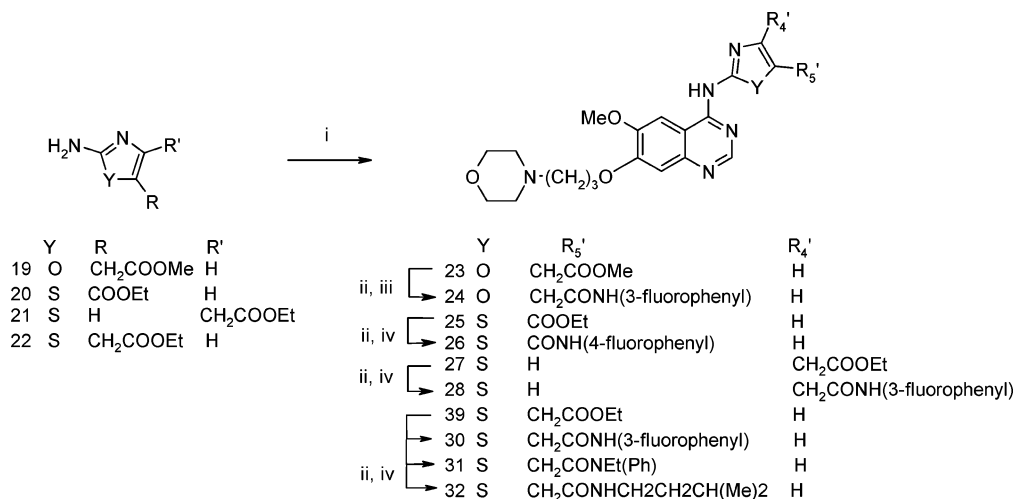
Chemistry. Our approach toward varying the C4 amino heterocycle of the quinazoline and its substituents is described in Schemes 1–7. We initially planned to synthesize these novel quinazolines by attempting to apply the well-known direct displacement of 4-chloroquinazolines by anilines.²⁶ However, we quickly realized that aminothiazoles, -oxazoles, -thiadiazoles, and -imidazoles do not undergo this reaction in preparatively useful yields. We decided, therefore, to utilize an alternative strategy for the synthesis of anilinoquinazolines^{27,28} (Schemes 2–4, 6, and 7) using the condensation of a cyanoimidate **6** under basic conditions with heterocyclic amines **9–11** to give the iminoquinazolines **12–14**. These iminoquinazoline intermediates readily undergo Dimroth rearrangements under basic conditions, leading to the target quinazolines **15–17** (Scheme 2). The intermediate carboxylic acid **17** was coupled with 4-fluoroaniline to give quinazoline amide **18**. In a related alternative approach, we also condensed amidine **7** with heterocyclic amines **19–22** under acidic conditions. The imino intermediates could not be isolated under these conditions, and the reaction led directly to the target quinazolines **23**, **25**, **27**, and **29** in good yields (Scheme 3). The mild experimental conditions used in the condensation of these five-membered ring heterocycles with the cyanoamidines proved extremely useful and versatile, allowing the presence of various functionalized substituents on the heterocycle as well as on the cyanoamidine. Saponification of

Scheme 1^a

^a (i) 4-(3-Chloropropyl)morpholine/DMF/K₂CO₃/80 °C/20 h; (ii) NH₂OH, HCl/AcOH, AcONa/reflux/18 h; (iii) HNO₃/AcOH/20 °C/20 h; (iv) Na₂S₂O₄/Bu₄NCl/CH₂Cl₂/H₂O/20 °C/20 h; (v) CH(OMe)₃/p-Tol SO₃H, cat./80 °C/6 h; (vi) DMF/DMA/105 °C/6 h.

Scheme 2^a

^a (i) 6/NaH/DMF/75 °C/1 h (for **9**, **10**) or 6/NaH/DMF/100 °C/3.5 h (for **11**); (ii) MeNH₂, AcOH/MeOH/75 °C/1 h (for **12**, **13**) or NaOH/MeOH/80 °C/1.5 h (for **14**); (iii) 4-fluoroaniline/HATU/DMF/DIEA, then Me₂NH/MeOH.

Scheme 3^a

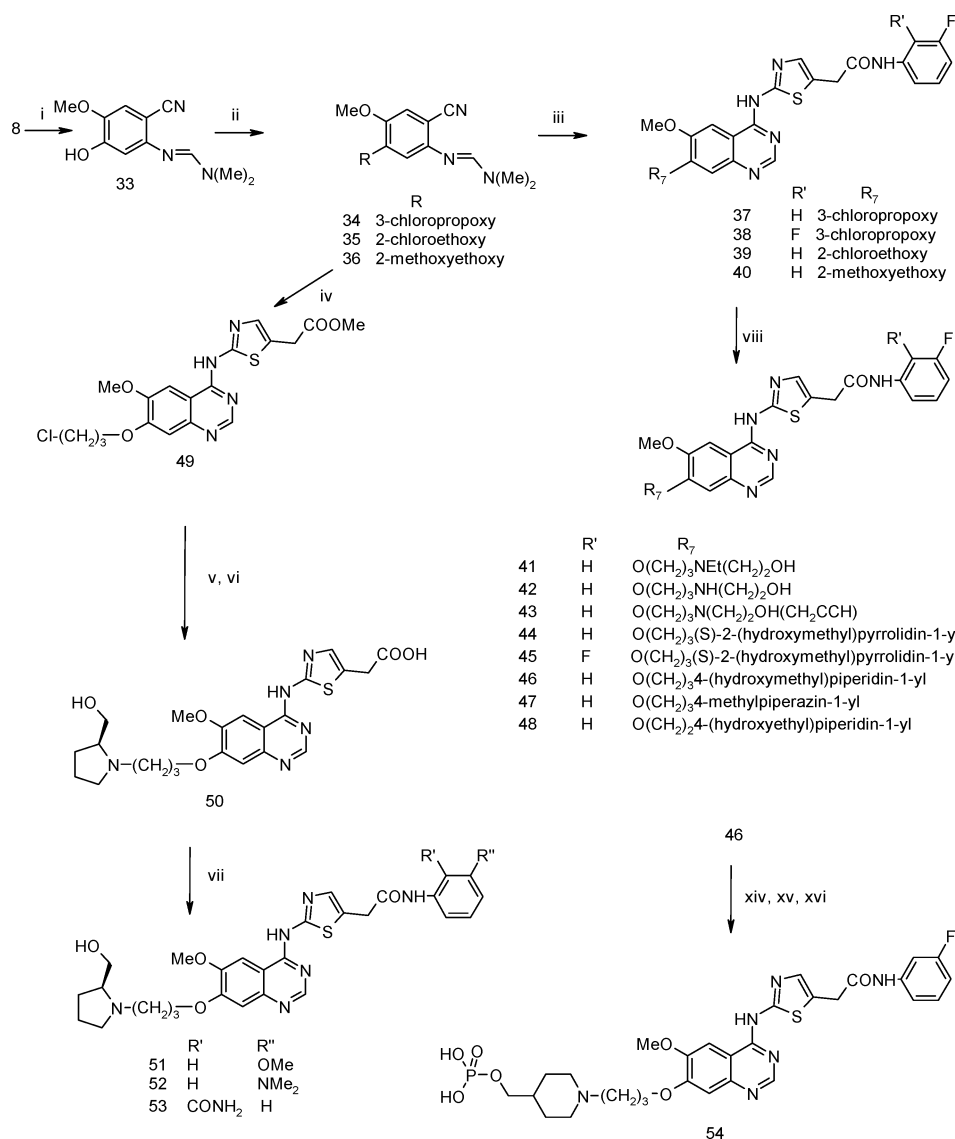
^a (i) 7/AcOH/reflux; (ii) NaOH/MeOH; (iii) 3-fluoroaniline/2-hydroxypyridine *N*-oxide/EDCI/DIEA/DMA; (iv) amine/HATU/DIEA/DMF.

the esters **23**, **25**, **27**, and **29**, followed by coupling with substituted anilines led to the target compounds **24**, **26**, **28**, and **30–32** (Scheme 3). The precursor imidate **6** and amidines **7** and **8** were obtained starting with aldehydes **1** in a straightforward multistep synthesis, which could be carried out on a kilogram scale (Scheme 1).

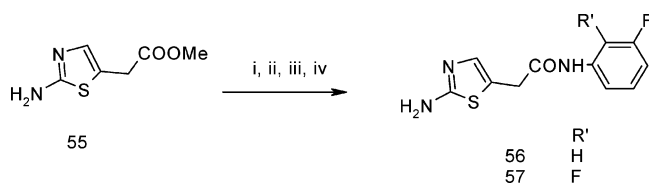
The compounds prepared in order to understand the effect of substitution on the C7 side chain of the quinazoline and the substitution around the aromatic ring are described in Scheme 4. Amidine **8** was debenzylated and the resultant phenol **33** was alkylated with chlorobromo alkyl halides to give the key cyanoamidines **34** and **35** (Scheme 4). Compound **34** was condensed with thiazole ester **55** to give the useful intermediate **49**. This versatile compound could be further elaborated at C7 by displacement of the chlorine with amine

nucleophiles as well as on the thiazole ring by coupling the corresponding carboxylic acid **50** with anilines to give the acetanilides **51–53**. Alternatively, the cyanoamidines **34** and **35** could also be condensed directly with thiazole amides **56** and **57** (Scheme 5) to give the intermediate quinazolines **37–39**. Subsequent nucleophilic substitution of the C7 chloropropoxy/chloroethoxy chains led to compounds **41–48** possessing diverse amino substituents on this side chain. The versatility of the key amidine **33** is further illustrated by its ready condensation with 1-bromo-2-methoxyethane to give the amidine **36**, which could in turn be condensed with thiazole amide **56** to give the quinazoline **40**.

Finally, to explore the replacement of the amide linker, a similar strategy was adopted. Amidine **34** was condensed with aminothiazoles **59** and **60** (Scheme 6) and **64** and **65** (Scheme

Scheme 4^a

^a (i) TFA/reflux; (ii) 1-chloro-3-bromopropane, 1-bromo-2-chloroethane or 1-methoxy-2-bromoethane/Cs₂CO₃/CH₃CN/80 °C/2 h; (iii) **56**, **57**/AcOH/reflux; (iv) **55**/AcOH/reflux (for **34**); (v) (S)-2-(hydroxymethyl)pyrrolidine/DMA/90 °C/2.5 h; (vi) NaOH/EtOH; (vii) aniline/2-hydroxypyridine *N*-oxide/EDCI/DIEA/50 °C/20 h; (viii) amine/NMP/KI (DMA/60 °C/48 h, for **48**); (xiv) Et₂NP(OtBu)₂/DMA/20 °C/2 h; (xv) H₂O₂/−10 °C/5 min; (xvi) HCl/dioxane/20 °C/20 h.

Scheme 5^a

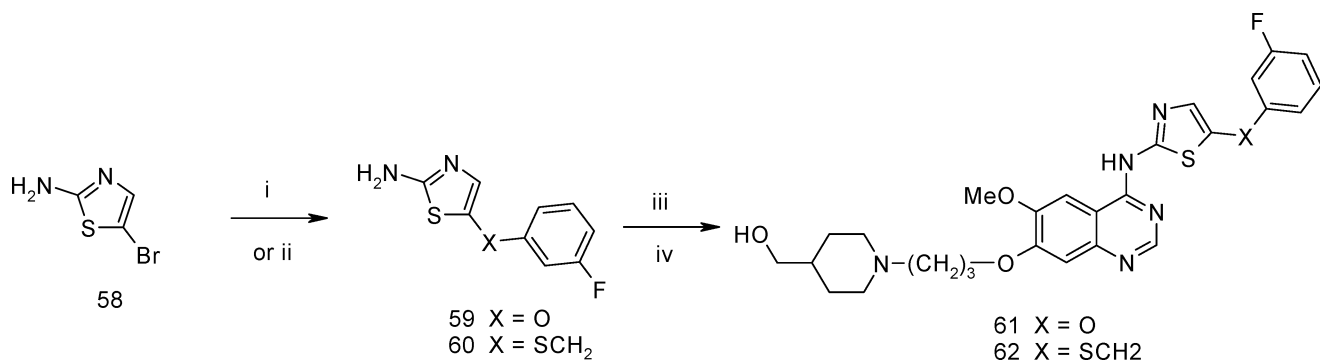
^a (i) Ph₃CCl/Et₃N/CH₂Cl₂/20 °C/2.5 h; (ii) NaOH/EtOH/20 °C/2.5 h; (iii) aniline/HATU/DIEA/DMF/50 °C/18 h; (iv) HCOOH/H₂O/60 °C/1.5 h.

7) to give the corresponding quinazolines **61**, **62**, **66**, and **67** after substitution of the side chain with the appropriate nucleophilic amine.

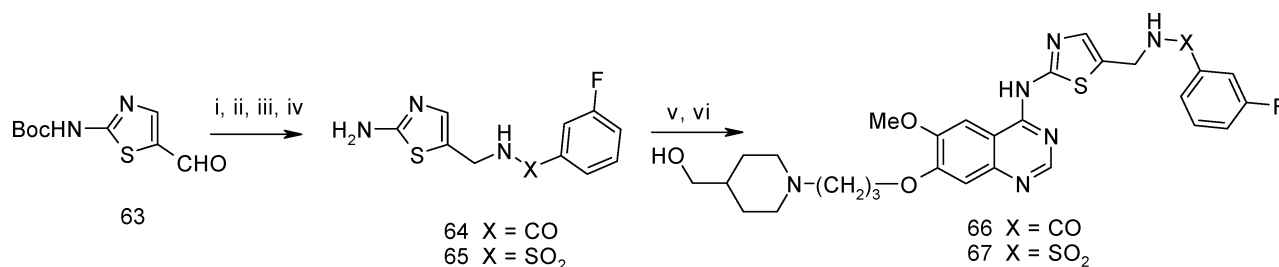
Results and Discussion

A number of analogues of ZM447439 where the central phenyl ring has been substituted for five-membered ring heterocycles have been widely explored.^{29,30} The Aurora kinase enzyme and cellular activities of a representative set of these compounds, showing the pertinent SAR, is summarized in Table 1.

The 2-aminothiazole series, e.g., compound **26**, retained affinity for the Aurora kinases and showed cellular activity similar to ZM447439, although other five-membered ring heterocyclic analogues displayed a reduction in binding affinity.³¹ In the case of the related 2-aminothiadiazole and 2-aminothiophene series, the compounds showed similar activity to the 2-aminothiazoles but displayed poorer physicochemical properties and/or lower chemical stability. 3-Aminopyrazole³⁰ substitution on the quinazoline gave very potent Aurora kinase inhibitors, and these compounds will be described separately. The replacement of the central six-membered phenyl ring by five-membered heterocycles modulates the relative orientation and conformation of the quinazoline and the benzamido moieties that exist in M447439. However, the sustained binding affinity observed in these series suggests that these changes can be accommodated by the enzyme, either because of a conformational flexibility of the kinase in that region or because the selectivity pocket is rather large. This suggested that improvements in selectivity and potency might be achievable by introducing further conformational change. Of the many com-

Scheme 6^a

^a (i) 3-Fluorophenol/Cs₂CO₃/CH₃CN; (ii) (3-fluorophenyl)methanethiol/NaH/CH₃CN; (iii) **34**/AcOH/reflux; (iv) 4-(hydroxymethyl)piperidine/NMP/KI.

Scheme 7^a

^a (i) NH₂OH, HCl/EtOH/Py; (ii) Zn/AcOH/AcOEt; (iii) 3-fluorobenzoyl chloride/CH₂Cl₂/Et₃N or 3-fluorobenzoyl chloride/Py/0 °C/3 h; (iv) CH₂Cl₂/TFA; (v) **34**/AcOH reflux; (vi) 4-(hydroxymethyl)piperidine/NMP/KI.

pounds prepared in this area, one series, where an extra methylene unit had been inserted between the amide carbonyl and the five-membered heterocyclic ring, e.g., compound **30**, stood out in terms of potency against Aurora A and B. Furthermore, when compounds containing this novel linking group were tested in a cellular assay, the increase in enzyme potency was found to translate into increased potency in cells.

Two interesting pieces of SAR came out of this initial work that are worthy of further discussion. First, there is a clear preference for the position of the substituent on the thiazole ring, with the C4 substituted compound **28** showing a 100-fold decrease in cellular activity compared with the C5 substituted compound **30** (Table 1); second, the acetanilide series is vastly superior in terms of cellular activity compared with the formylanilide series, e.g., compare compounds **30** and **26**, respectively. Each of these intriguing pieces of SAR will now be discussed further.

The free rotation around the methylene bond of the acetanilide group and around the NH–C2' bond (Table 2) in compounds such as **28** and **30** might have been expected to allow the large terminal aryl ring to occupy a similar region of space, regardless of whether it was attached through the C4 or C5 position of the thiazole. However, the large difference in activity seen between compounds **28** and **30** suggests the existence of a privileged orientation of the heterocycle relative to the quinazoline ring system that requires the side chain to be in the C5 position of the thiazole to optimally occupy the hydrophobic selectivity pocket. While a crystal structure of Aurora A complexed with a related pyrimidinoquinazoline has been solved,³² it was not possible to cocrystallize a thiazole derivative into Aurora A, although docking studies have been carried out.

In an attempt to rationalize the biological activity of the thiazole series, we have analyzed the conformation of a heterocyclic model system using ab initio molecular orbital calculations.³³ Our results show that the thiazole ring adopts a strongly preferred orientation coplanar to the quinazoline ring,

with the sulfur atom located on the same side as the quinazoline N3 (Table 2). This can be explained not only by the electronic repulsion of the quinazoline and the thiazole nitrogen atoms, but also by the stabilizing effect created by the polar interaction between the partial positive charge of the thiazole sulfur atom and the partial negative charge on the quinazoline N3. Similar stabilizing interactions in structurally closely related compounds have been reported recently.³⁴ In the model used, these effects favor this conformation by 17.16 kcal/mol over the other planar conformation (Table 2). The direct consequence of the existence of such a privileged stable conformation is the nonequivalence of the C4 and the C5 thiazole positions. The excellent potency of the C5-substituted thiazoles and these calculated data suggest that the most stable and bioactive conformations are closely related and that the preferred position for a substituent is in the C5 position.

The oxazole **24** is only weakly active against these kinases, in contrast to the thiazole analogue **30** (Table 1). In this case, the preferred conformation is calculated to show a torsional angle of 28° between the oxazole and the quinazoline rings (Table 2). For this compound, the calculated energy difference between the low-energy state and the coplanar, presumably bioactive state, with the oxygen atom of the oxazole group on the same side as the quinazoline N3, is quite small (1.59 kcal/mol) and cannot alone explain the poor activity of the oxazole series.

The 2-aminoimidazole moiety in compound **18** (Table 1) may be expected to stabilize the coplanar state by the likely existence of an internal H-bond between the imidazole NH and the quinazoline N3 and thus freeze the imidazole ring in the bioactive conformation, as illustrated by form "A" in Table 2. However, compound **18** is much less active against both Aurora A and B kinases than the thiazole **26** (Table 1). Ab initio molecular orbital calculations³³ showed the tautomeric "B" form in our model to be 1.69 kcal/mol more stable than the A form, consequently giving the side chain an unfavorable orientation.

Table 1. Summary of SAR in Thiazoloylquinazoline Series

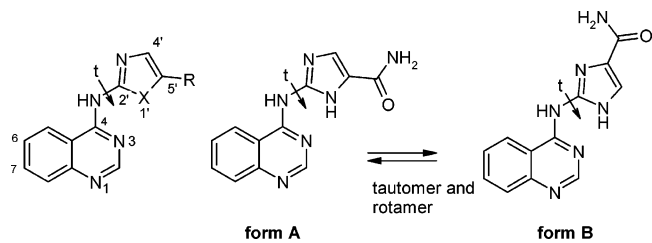
No.	Structure	Enzyme IC ₅₀		Cell ^c IC ₅₀ μmol	No.	Structure	Enzyme IC ₅₀		Cell ^c IC ₅₀ μmol
		A ^a	B ^b				A ^a	B ^b	
15		0.043	0.133	1.1	44		<0.001	<0.001	0.004
16		0.006	0.063	1.9	45		0.002	0.002	0.001
26		0.001	0.049	0.6	51		0.106	0.005	1
28		0.578	0.012	0.2	52		0.483	0.048	0.6
30		<0.001	<0.001	<0.001	53		0.452	0.282	>10
18		>1	>1	>10	40		0.001	0.008	0.01
24		0.472	0.341	1	42		0.005	0.001	0.08
31		0.055	0.286	2.3	41		<0.001	<0.001	<0.001
32		0.158	0.005	0.4	43		<0.001	<0.001	0.02
61			<0.001	0.2	47		<0.001	<0.001	0.002
62		<0.001	<0.001	0.4	46		<0.001	0.007	0.005
66		0.111	0.136	2.8	48		<0.001	<0.001	0.019
67		0.012	0.028	0.8					

^a Concentration to inhibit by 50% the phosphorylation of a biotin tetra-LRRWSLG peptide substrate by Aurora A. ^b Concentration to inhibit by 50% the phosphorylation of a biotin tetra-LRRWSLG peptide substrate by Aurora B-INCENP complex. Values are averages from at least two independent dose-response curves; variations are generally $\pm 15\%$. ^c Concentration to inhibit by 50% the level of phosphorylation of histone H3 in SW620 cells. Values are averages from at least two independent dose-response curves; variations are generally $\pm 15\%$.

However, again the energy difference between the two tautomeric forms is small and additional reasons to explain the inactivity have to be sought. The reasons for the weak activity of the oxazole and imidazole series compared with the thiazole series remain elusive, but we may anticipate that unfavorable lipophilicity and electron density play key roles. Indeed, the selectivity pocket is comprised of lipophilic residues, in particular, the gatekeeper residue (Leu210) at the entrance of

the pocket and presumably close to the heterocycle. Moreover, the position of the acetamide chain may be affected by the changes in the geometry between sulfur, oxygen, or nitrogen containing heterocycles.

The exquisitely high cellular activity of the thiazoloquinazolines with an acetamide substituent, e.g., compound **30**, compared with the analogous formamide compounds, e.g., **26**, led us to attempt to rationalize this interesting finding.

Table 2. Calculated Conformational Preference for the Thiazole, Oxazole, and Imidazole Models


X	R	conformation	$\Delta E(\text{RHF}/6\text{-}31\text{G}^*)^a$ (kcal/mol)
S	H	$t = 0^\circ$, S on the side of N3	0
S	H	$t = 180^\circ$, N on the side on N3	17.16
O	H	$t = 0^\circ$, O on the side of N3	1.59
O	H	$t = 180^\circ$, N on the side of N3	2.09
O	H	$t = 28^\circ$, O on the side of N3	0
NH	CONH ₂	form A, $t = 0^\circ$, NH on the side of N3	1.69
NH	CONH ₂	form B, $t = 180^\circ$, NH on the side of N3	0

^a Energy difference between the different conformers are calculated with the restricted Hartree–Fock (RHF) model³⁶ at the 6-31G* level.

It is clear that the complete acetanilide substitution on the thiazole ring is crucial for highly potent cellular activities. Increasing the lipophilicity of the thiazole C5 substituent with nonfunctionalized alkyl chains, e.g., compounds **15** and **16** (Table 1), led to compounds with activity against the Aurora enzymes, but with only weak cellular activity. The weak cellular activity of acetamide **32** (Table 1) shows that the amide group alone is insufficient to achieve cellular activity and that the aromatic ring of the acetanilide moiety must play an important role. Substitution of the free amidic NH is not tolerated, e.g., compound **31** (Table 1). Ether and thiomethyl linker groups, e.g., compounds **61** and **62**, respectively (Table 1), again gave compounds with very good enzymatic activity but poor cellular potency. Although the physicochemical properties of compounds **15**, **16**, **31**, **32**, **61**, and **62** are different, we believe that the absence of the key binding interactions mediated by the acetanilide linker group could explain the absence of any significant cellular activity in these compounds. The reverse amide and sulfonamide linking groups, e.g., in compounds **66** and **67**, respectively (Table 1), are not tolerated, giving weak enzyme and cellular activities.

Different crystal structures of Aurora A in an active or inactive conformation with ATP analogues have been published.^{32,35–37} In the in-house crystal structure, Aurora A forms a complex with a small molecule inhibitor from the pyrimidinoquinazoline series (Figure 1) and adopts an inactive conformation with displacement of the DFG motif in the activation loop where the F residue is shifted out (DFG-out).³² It also shows the existence of a dual interaction between a conserved Lys (K162), one of the pyrimidine nitrogens, and the carbonyl oxygen of the amide, suggesting an important role for this carbonyl in the activity of the compound (Figure 1). Similar binding interactions may exist with the acetanilide chain; however, the interposed methylene and the inversion of the amide may lead to a different binding mode within the hydrophobic pocket that could translate into better cellular potency. In the absence of a crystal structure of such a complex, we have performed modeling studies on the acetanilide analogue. Unsurprisingly, the more flexible acetanilide side chain adopts a near-perpendicular orientation relative to the thiazole, very different from the planar ensemble observed in the pyrimidinoquinazoline amide series. This bent molecular conformation is reminiscent of the bioactive conformation of

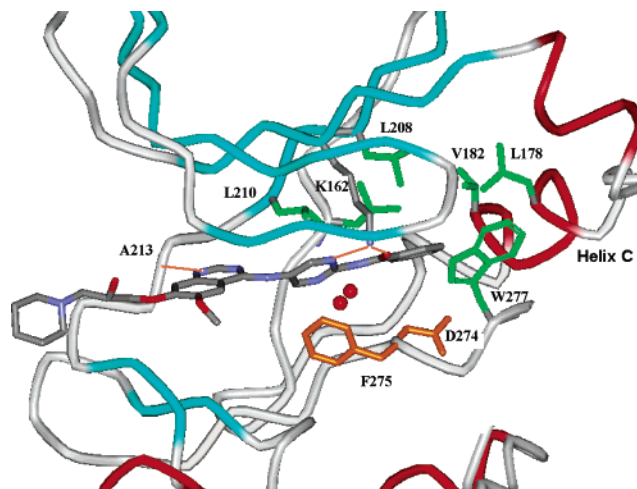


Figure 1. Crystal structure of the 4-aminopyrimidinoquinazoline derivative **68** bound to Aurora A (pdb accession code 2c6e).³² The protein is presented as a tube diagram colored by secondary structure, with the side chains of key lipophilic residues colored in green (carbon chain of Q185 and E181 on helix C have been omitted for clarity). The inhibitor is represented in stick form and colored by element. The quinazoline ring binds into the purine site of the ATP binding site and makes a highly conserved hydrogen bond with the backbone NH of A213 (orange line). The pyrimidine side chain enters deeply into the hydrophobic pocket (green amino acids). Conserved K162 residue makes a double hydrogen bond with one pyrimidine nitrogen and with the carbonyl oxygen of the amide link (orange lines). The other pyrimidine nitrogen and the amide NH interact with the protein backbone via two water molecules (red balls). Overall the conformation of the inhibitor is extended and very flat. The kinase is in a DFG-out conformation, as illustrated by the position of D274 and F275 (colored in orange).

inhibitors such as STI-571 (Gleevec),³⁸ BIRB-796,³⁹ or BAY43-9006⁴⁰ bound to their respective targets c-Abl, P38, or c-Raf kinase (Figure 2). This suggests to us that the interactions of the acetanilide chain with Aurora A could be similar to the interactions of the side chains of these inhibitors that have been shown to bind strongly to an inactive conformation of the enzyme characterized by a considerable shift of the F residue in the DFG motif. In these structures, the movement of the F residue creates a large hydrophobic pocket in the kinase and the inhibitors side chain can then insert deeply into this pocket. Importantly, a characteristic hydrogen-bond pattern involving an amide or urea group of the inhibitor, the main chain nitrogen of the conserved Asp (of the DFG motif), and the carboxylate side chain of the catalytic Glu (on helix C) strongly contributes to the binding affinity for the inactive conformation. Docking of compound **46** in our Aurora A structure shows that the enzyme could accommodate the acetanilide chain to form these particular interactions. Catalysis in the enzymatic assay is performed by an active DFG-in conformation, whereas in the cell assay both DFG-in and DFG-out conformations are present. We suggest that the acetanilide derivatives possess the structural features required to bind efficiently to the DFG-out conformations, which may account for the significant improvement in cellular over enzymatic potency we observed. Given the high sequence identity between the A and B forms (~70% on the kinase domain), we believe that the arguments we put forward for Aurora A may also be valid for Aurora B. A crystal structure of Aurora B in complex with its activator INCENP and the inhibitor hesperadin has been recently published.⁴¹ However, hesperadin binds to an active conformation of Aurora B which differs markedly from our Aurora A crystal structure and from

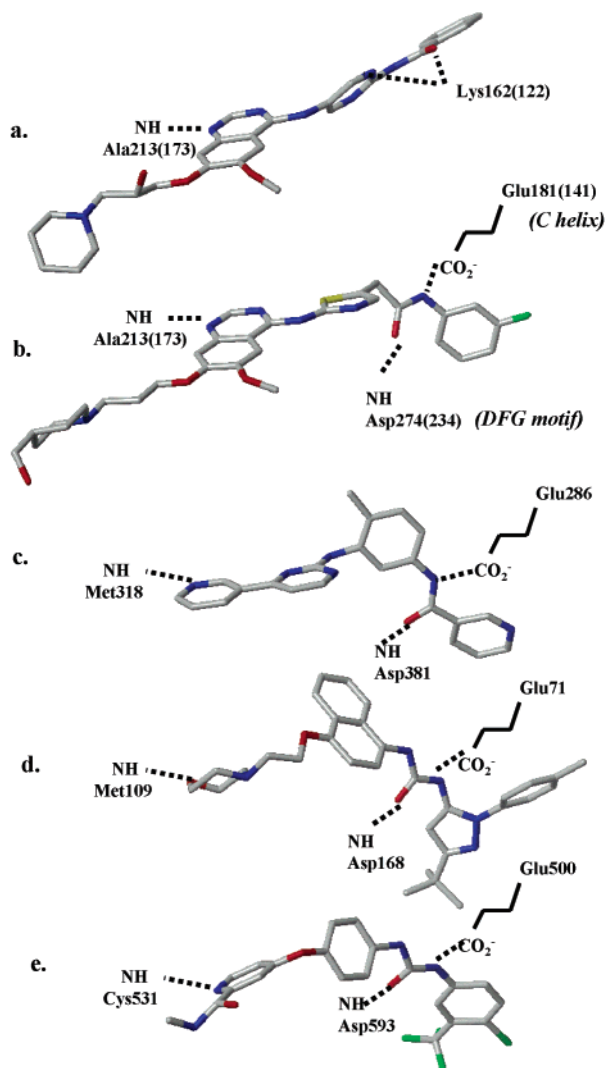


Figure 2. Comparison of the conformation adopted by compound **68** (a, crystal structure) and **46** (b, model) when bound to Aurora kinase A (numbering of corresponding residues in Aurora B are in brackets). The acetanilide chain in compound **46** adopts a clearly different conformation to that of the side chain of compound **68** but very close to the conformation of the side chain of Gleevec (c), BIRB-796 (d), or BAY43-6009 (e) when bound to the DFG-out conformation of their respective target kinase (c-Abl, P38, and c-Raf). Key hydrogen bonds in the purine binding site and in the large hydrophobic pocket are illustrated as dotted lines.

the structures of Gleevec or related inhibitors bound to the inactive form of their target kinases.

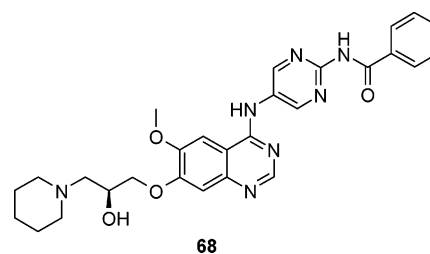
A study of the substitution of the anilide ring in compounds such as **44** was undertaken to optimize the potency, physical properties, and selectivity of our compounds. A number of these substitutions have been described in a patent application.²⁹ The crystal structure of Aurora A complexed with the pyrimidinoquinazoline derivative **68** reveals that the terminal aromatic ring of the inhibitor binds near the bottom of the hydrophobic pocket of the kinase and is mainly surrounded by hydrophobic residues (Figure 1). Although the acetanilide chain may bind differently in the 4-aminothiazoloquinazoline series, we have also observed that lipophilic substituents on the anilide ring are advantageous in terms of potency, e.g., compounds **44** and **45**, whereas compounds with hydrophilic substituents had vastly reduced binding affinity, e.g., compounds **51–53** (Table 1). Interestingly, the inhibitors STI-157, BIRB-796, and BAY43-9006 also possess a lipophilic aromatic ring next to the amide or urea

Table 3. Physicochemical and Pharmacokinetic Properties for Compound **46** and the Phosphate Derivative **54**

R	solubility, mg/mL	% free drug	rat pharmacokinetics		
			volume, L/kg	clearance, mL/min/kg	half-life, h
46 H	0.035 ^a	2.4 ^c	1.8	16.6	5.0
54 P(O)OH ₂	10b				

^a pH 7.4 at 25 °C in phosphate buffer. ^b pH 9.0 at 25 °C in 0.3 mol Tris buffer. ^c Rat serum albumin at 37 °C.

link, binding probably to the same region of the kinase (Figure 2). This suggests to us that some of these lipophilic interactions are conserved, but we cannot discard the possibility that residue Trp277 (Trp237 in Aurora B), contiguous to the DFG motif and only found in Aurora A and B, plays an additional key role in these interactions.



Modification of the C7 position of quinazoline kinase inhibitors is known to profoundly influence activity and selectivity.^{42–45} The physicochemical properties of quinazoline compounds can also be largely influenced by the introduction of hydrophilic and basic groups on the quinazoline.⁴³ The C7 substituent accesses the solvent channel, explaining why a wide range of strongly polar groups is tolerated (e.g., compounds **41**, **42**, **43**, **46**, and **47**; Table 1), provided that a suitable linear spacer is included between the solubilizing group and the quinazoline. A three-carbon linker is generally optimal, although two-carbon linkers are also tolerated, e.g., compound **48**. The spacer occupies a more sterically crowded region, where it makes a hydrophobic interaction with the protein surface; thus, hydrophobic groups also give excellent binding affinities, e.g., compound **40**, but result in poorer physicochemical properties, especially solubility. Generally, increasing the lipophilic nature of the quinazoline C7 substituent increases cellular potency, but solubility decreases and binding to plasma proteins increases.

Variation of the quinazoline C7 side chain allowed fine-tuning of the overall properties of the compounds. Compound **46** was chosen for further study as it shows a good balance between enzyme and cell potency and physicochemical and pharmacokinetic properties (Table 3). Compound **46** has moderate lipophilicity ($\log D_{7.4} = 3.2$), does not significantly inhibit the hERG receptor ($IC_{50} > 10 \mu\text{mol}$), has a free drug level of 2.4% when measured in rat serum albumin, and has low clearance in rodents with a moderate volume of distribution, giving it excellent exposure when administered by either intraperitoneal (ip) or intravenous (iv) routes. SW620 cells treated with compound **46**, for 24 h, showed both a dramatic accumulation of 4n cells (consistent with a failure of cytokinesis) and a complete inhibition of phosphorylation of histone H3 in a dose-

Table 4. Selectivity Profile (IC_{50} , μmol^a) in a Panel of Kinases^b of Compound **46**

CDK2	CSK	EGFR	FAK	FGFR	IGFR	JAK3	JNK1A	KDR	P38A	PKA	SRC
62	21	0.8	4	8	13	25	>100	1	>100	>100	3

^a ATP concentrations used are $\leq K_m$ of the kinase. ^b Experimental details for in vitro receptor TK inhibition assays can be found in the Experimental Section.

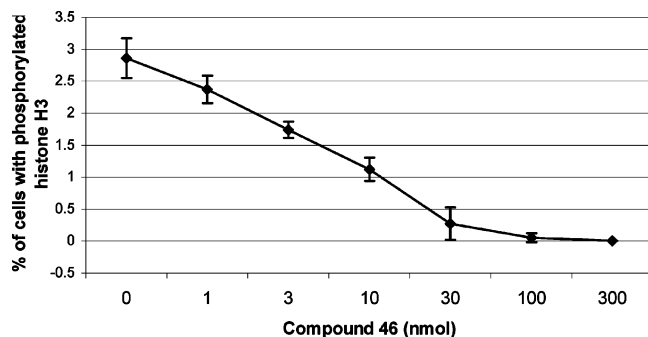


Figure 3. Inhibition of the phosphorylation of histone H3 by compound **46**, a cellular substrate for Aurora B in SW620 human colon tumor cells. Compound **46** was shown to be a potent suppressor of histone H3 phosphorylation, causing a dose-related decrease in cellular levels of phospho-histone H3 ($IC_{50} = 5.1 \text{ nmol}$, $n = 2$) consistent with inhibition of Aurora kinases.

dependent manner (Figure 3). Compound **46** also demonstrates a very potent antiproliferative effect in SW620 cells, with an $IC_{50} = 0.002 \mu\text{mol}$. In a panel of serine-threonine and tyrosine kinases, compound **46** shows excellent specificity for the Aurora kinases (Table 4). Reassuringly, the phenotype seen for compound **46** is identical to those reported for specific inhibition of Aurora kinase activity reported in other systems.^{8,24,25}

To provide tools to explore the in vivo effects of long-term exposure of an Aurora kinase inhibitor, it was necessary to

identify compounds with high aqueous solubility ($>10 \text{ mg/mL}$) suitable for infusion studies. Compound **46** has low solubility (Table 3), but the presence of a hydroxyl group in the quinazoline C7 side chain, in compounds such as **46**, allowed suitable prodrugs to be prepared. The phosphate derivative of compound **46** (compound **54** in Table 3) was prepared and found to have excellent solubility in pH-adjusted vehicles and, importantly, to undergo rapid conversion to the parent drug in vivo ($t_{1/2} = 0.7 \text{ h}$ in mouse plasma).

The pharmacodynamic (PD) consequences of Aurora kinase inhibition by compound **46** was tested in nude mice bearing established ($>0.2 \text{ cm}^3$ volume) subcutaneous SW620 human colorectal carcinoma xenografts. The phosphate derivative **54** was dosed at 67 mg/kg/day , as a constant infusion for 48 h via an osmotic subcutaneous minipump (Figure 4). The results are striking in tumor sections immunostained for phospho-histone H3 expression (Figure 4a,b). Analysis of phospho-histone H3 stained cells using a scanning microscope (Figure 4c) indicated a 32% ($p < 0.01$) reduction in phospho-histone H3 positive cells in the compound-treated sections versus vehicle control.

Conclusion

In the course of this work, our efforts have focused on the design and preparation of Aurora family specific kinase inhibitors starting from the anilinoquinazoline lead ZM447439. Our goals were to enhance the potency of this compound while its

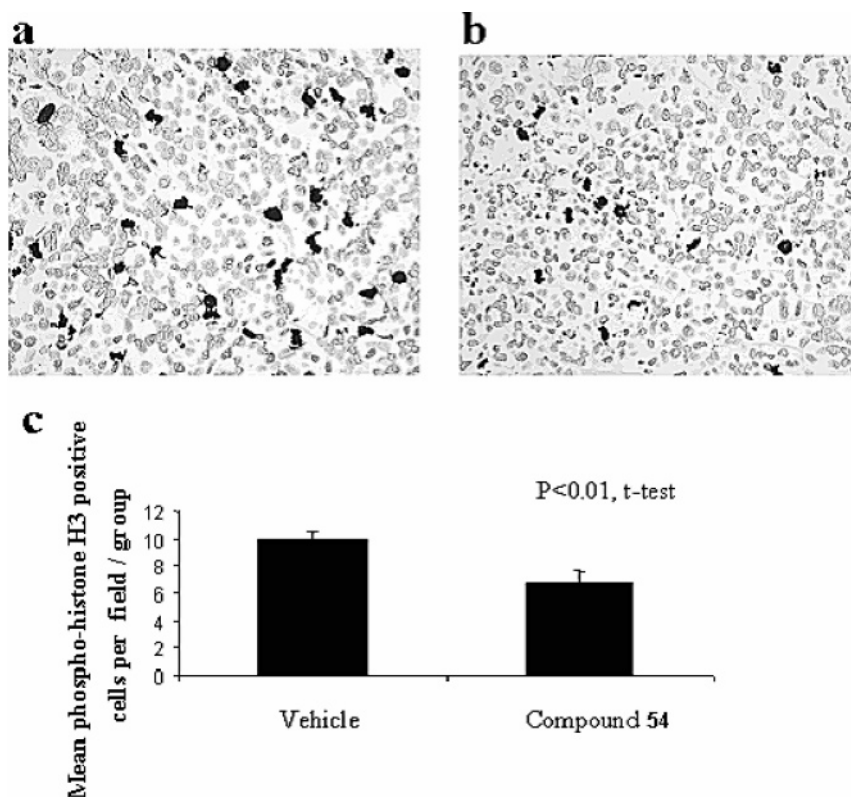


Figure 4. Pharmacodynamic effect of compound **54** on human colorectal carcinoma SW620 in nude mice. Compound **54** (67 mg/kg/day) was dosed as a continuous infusion via an subcutaneous osmotic minipump for 48 h. Phospho-histone H3 immunostained tumors: (a) vehicle control and (b) compound **54** treated. (c) Analysis by scanning microscopy of phospho-histone H3 staining. Data are mean \pm SEM from five separate experiments ($n = 3$ animals per group, 1 tumor section per animal, 6 fields per tumor).

selectivity was maintained and to improve on its physicochemical properties. We discovered a novel series of potent and specific Aurora A and B inhibitors possessing 2-aminothiazole at C4 of the quinazoline ring. The compounds synthesized displayed high selectivity against a panel of serine-threonine and tyrosine kinases. We found that a lipophilic substituent attached to the thiazole ring greatly increases the *in vitro* potency of the compounds. The position of attachment of this substituent and the nature of the linker group is of key importance for high cellular potency, the acetanilide group at C5 of the thiazole giving compounds with very high potency in cells. Theoretical *ab initio* calculations helped us to rationalize some of these findings.

Experimental Section

General Methods. Melting points were determined on a Leica melting point apparatus and are uncorrected. ¹H NMR spectra were recorded on an EX 400 JEOL FT NMR spectrometer. Chemical shifts are reported as δ values downfield from internal TMS in appropriate organic solutions. The purity and the structures of the final products were confirmed by LC-MS on a Waters 996 photodiode array detector system using the following conditions: Column, Symmetry C-18; solvent A, water 0.1% formic acid; Solvent B, CH₃CN; flow rate, 2.5 mL/min; run time, 4.5 min; gradient, from 0 to 100% solvent B; mass detector, micro mass ZMD. The IR spectra were recorded on a Bruker Vector IR spectrometer. Combustion analyses (C, H, N) were performed with a Carlo Erba EA1108 analyzer, and the results agreed with the theoretical values to within $\pm 0.4\%$. Chromatographic purifications were by flash chromatography using 40–63 μ m Merck silica gel.

Synthetic Chemistry. 3-Methoxy-4-(3-morpholin-4-ylpropoxy)-benzonitrile (2). **Step 1.** 4-Hydroxy-3-methoxybenzaldehyde (279 g, 1.8 mol) was solubilized in DMF (1.5 L) in the presence of K₂CO₃ (376 g, 2.7 mol). 4-(3-Chloropropyl)morpholine (330 g, 2 mol) was slowly added to the mixture over 30 min and the mixture was heated at 80 °C for 20 h. This reaction was cooled, the insoluble salts were filtered, and the DMF solution was concentrated. The residual oil was dissolved in EtOAc (2 L), and the solution washed with H₂O (3 \times 1 L), dried, and concentrated to give 3-methoxy-4-(3-morpholin-4-ylpropoxy)benzaldehyde as a beige solid (365 g, 73%): ¹H NMR (DMSO-*d*₆) δ 1.93 (t, 2H), 2.38 (m, 4H), 2.43 (t, 2H), 3.58 (t, 4H), 3.85 (s, 3H), 4.14 (t, 2H), 7.19 (d, 1H), 7.4 (d, 1H), 7.55 (dd, 1H); MS ESI⁺ *m/z* 280 (M + H)⁺.

Step 2. 3-Methoxy-4-(3-morpholin-4-ylpropoxy)benzaldehyde (362.5 g, 1.3 mol) was dissolved in anhydrous AcOH (1.6 L). NaOAc (213 g, 2.6 mol) and NH₂OH·HCl (180 g, 2.6 mol) were added to the solution, which was heated at 130 °C for 18 h. The mixture was cooled, diluted with H₂O (2 L), and extracted with CH₂Cl₂ (4 \times 1 L). The organic phases were combined, dried, and evaporated to give **2** (358 g, 100%): ¹H NMR (DMSO-*d*₆, TFA) δ 2.19 (2H), 3.13 (t, 2H), 3.31 (t, 2H), 3.52 (d, 2H), 3.68 (t, 2H), 3.85 (s, 3H), 4.02 (d, 2H), 4.17 (t, 2H), 7.15 (d, 1H), 7.42 (m, 2H); MS ESI⁺ *m/z* 277 (M + H)⁺.

2-Amino-5-methoxy-4-(3-morpholin-4-ylpropoxy)benzonitrile (4). **Step 1.** **2** (358.8 g, 1.3 mol) was dissolved in anhydrous AcOH (600 mL) and slowly added to a cool (5–10 °C) solution of HNO₃ (69%, 1.7 L) at such a rate so that the temperature of the mixture did not exceed 15 °C. The mixture was then stirred at room temperature overnight and basified at 0 °C with KOH (10 N). The precipitate was filtered, suspended in CH₂Cl₂ (4 L), and washed with H₂O (2 \times 2 L). The organic phase was dried and concentrated to give 5-methoxy-4-(3-morpholin-4-ylpropoxy)-2-nitrobenzonitrile (193 g, 46%): ¹H NMR (DMSO-*d*₆) δ 1.92 (m, 2H), 2.35 (m, 4H), 2.41 (t, 2H), 3.57 (t, 2H), 3.97 (s, 3H), 4.24 (t, 2H), 7.69 (s, 1H), 7.87 (s, 1H); MS ESI⁺ *m/z* 322 (M + H)⁺.

Step 2. 5-Methoxy-4-(3-morpholin-4-ylpropoxy)-2-nitrobenzonitrile (192 g, 0.6 mol) was dissolved in CH₂Cl₂. Tetrabutylammonium chloride (115 g, 0.41 mol) was added followed by the slow addition of a solution of Na₂S₂O₄ (734 g, 3.6 mol) in H₂O

(2.6 L), resulting in a gentle reflux. The mixture was stirred for 3 h at room temperature and basified (pH 12) at 0 °C with a solution of NaOH (2 N). The organic phase was recovered and the aqueous phase extracted with CH₂Cl₂ (2 \times). The combined organic phases were treated with an ethereal solution of HCl, and the precipitated solid was recovered and dissolved in H₂O. The aqueous phase was basified (pH 10.5) with NaOH (2 N) and extracted with EtOAc. The organic phase was dried and concentrated to give **4** (81 g, 47%): ¹H NMR (DMSO-*d*₆) δ 1.88 (t, 2H), 2.35 (m, 4H), 2.39 (t, 2H), 3.56 (m, 4H), 3.64 (s, 3H), 3.94 (t, 2H), 5.59 (s, 2H), 6.41 (s, 1H), 6.87 (s, 1H); MS ESI⁺ *m/z* 292.2 (M + H)⁺. Anal. (C₁₅H₂₁N₃O₃·0.2H₂O) C, H, N.

Methyl [2-Cyano-4-methoxy-5-(3-morpholin-4-ylpropoxy)-phenyl]imidiformate (6). **4** (2.91 g, 10 mmol) was solubilized in trimethylorthoformate (10 mL), PTSA (38 mg, 0.2 mmol) was added, and the mixture was heated at 80 °C for 6 h. The reaction mixture was cooled and concentrated, and the residue was triturated with Et₂O to give an orange solid (3.01 g, 90%): ¹H NMR (DMSO-*d*₆) δ 1.94 (m, 2H), 2.34 (m, 4H), 2.4 (t, 2H), 3.6 (t, 4H), 3.78 (s, 3H), 3.85 (s, 3H), 4.11 (t, 2H), 6.89 (s, 1H), 7.28 (s, 1H), 8.2 (s, 1H); MS ESI⁺ *m/z* 334.1 (M + H)⁺. Anal. (C₁₇H₂₃N₃O₄) C, H, N.

N'-[2-Cyano-4-methoxy-5-(3-morpholin-4-ylpropoxy)phenyl]-N,N-dimethylimidiformamide (7). **4** (2.91 g, 10 mmol) was suspended in toluene (50 mL), and DMF-DMA (1.79 g, 15 mmol) was added to the mixture, which was heated at 105 °C for 5 h in a Dean-Stark apparatus. The solution was concentrated and the residue triturated with Et₂O to give **7** as an off-white solid (3.4 g, 98%): ¹H NMR (DMSO-*d*₆) δ 1.86 (m, 2H), 2.3 (m, 4H), 2.4 (t, 2H), 2.95 (s, 3H), 3.05 (s, 3H), 3.56 (t, 4H), 3.72 (s, 3H), 4.07 (t, 2H), 6.72 (s, 1H), 7.08 (s, 1H), 7.89 (s, 1H); MS ESI⁺ *m/z* 347.2 (M + H)⁺.

6-Methoxy-N-(5-methyl-1,3-thiazol-2-yl)-7-(3-morpholin-4-ylpropoxy)quinazolin-4-amine (15). Imidate **6** (300 mg, 0.9 mmol) in DMF (4.5 mL) was reacted with **9**^{29,46} (113 mg, 0.99 mmol) in the presence of NaH (39.9 mg, 0.99 mmol) at 75 °C for 2 h to give intermediate **12**. AcOH (77 μ L, 1.35 mmol) was then added to the mixture at room temperature, followed by MeOH–Me₂NH (2 M, 90 μ L, 0.18 mmol), and the mixture was stirred at 75 °C for 1 h, resulting in formation of **15**. The solvent was evaporated and the residue was purified by silica gel chromatography, eluting with CH₂Cl₂:MeOH (95:5 to 90:10) to give **15** (300 mg, 80%): ¹H NMR (DMSO-*d*₆, TFA) δ 2.31 (t, 2H), 2.42 (s, 3H), 3.16 (t, 2H), 3.35 (t, 2H), 3.55 (d, 2H), 3.68 (t, 2H), 3.97 (s, 3H), 4.04 (d, 2H), 4.29 (t, 2H), 7.3 (s, 1H), 7.48 (s, 1H), 7.86 (s, 1H), 9.03 (s, 1H); MS ESI⁺ *m/z* 416.6 (M + H)⁺. Anal. (C₂₀H₂₅N₅O₃S·0.3H₂O) C, H, N.

2-[[6-Methoxy-7-(3-morpholin-4-ylpropoxy)quinazolin-4-yl]amino]-1H-imidazole-5-carboxylic Acid (17). **Step 1.** An analogous reaction to that described for the preparation of **15**, but starting with imidazole **11**^{29,46} (117 mg, 0.75 mmol) and heating at 100 °C for 3 h, afforded intermediate **14** (125 mg, 36%): ¹H NMR (DMSO-*d*₆, TFA) δ 1.32 (t, 3H), 2.3 (m, 2H), 3.15 (t, 2H), 3.34 (t, 2H), 3.55 (d, 2H), 3.68 (t, 2H), 3.98 (s, 3H), 4.03 (d, 2H), 4.33 (s, 2H), 4.37 (t, 2H), 7.49 (s, 1H), 8.11 (s, 1H), 8.2 (s, 1H), 8.65 (s, 1H); MS ESI⁺ *m/z* 457 (M + H)⁺.

Step 2. The rearrangement of **14** and saponification of the ester was carried out in one-pot by treating **14** (650 mg, 1.42 mmol) with NaOH (2 N) in MeOH at reflux for 2 h. Acidification followed by evaporation of the solvent gave **17** (609 mg, 100%): ¹H NMR (DMSO-*d*₆, TFA) δ 2.35 (m, 2H), 3.12 (m, 2H), 3.31 (m, 2H), 3.5 (m, 2H), 3.9 (m, 4H), 3.95 (s, 3H), 4.28 (t, 2H), 7.42 (s, 1H), 7.8 (s, 1H), 7.87 (s, 1H), 8.71 (s, 1H); MS ESI⁺ *m/z* 429.1 (M + H)⁺.

N-(4-Fluorophenyl)-2-[[6-methoxy-7-(3-morpholin-4-ylpropoxy)quinazolin-4-yl]amino]-1H-imidazole-5-carboxamide (18). The acid **17** (250 mg, 0.58 mmol) in DMF (4 mL) was reacted with 4-fluoroaniline (60 μ L, 0.58 mmol) in the presence of *O*-(7-azabenzotriazol-1-yl)-*N,N,N',N'*-tetramethyluronium hexafluorophosphate (222 mg, 0.58 mmol) and DIEA (150 μ L, 0.878 mmol) at 40 °C for 3 h. A solution of Me₂NH in MeOH (2 M, 1 mL) was added, and stirring was carried on for 3 h. The solvent was evaporated, and the mixture was purified by silica gel chromatog-

raphy, eluting with CH₂Cl₂:MeOH, NH₃ (3 N) (95:5) to give **18** (120 mg, 39%): ¹H NMR (DMSO-*d*₆, TFA) δ 2.29 (t, 2H), 3.17 (t, 2H), 3.36 (t, 2H), 3.55 (d, 1H), 3.69 (t, 2H), 3.96 (s, 3H), 4.04 (d, 2H), 4.27 (t, 2H), 7.22 (m, 3H), 7.74 (m, 2H), 7.82 (s, 1H), 8.07 (s, 1H), 8.76 (s, 1H); MS ESI⁺ *m/z* 522.1 (M + H)⁺. Anal. (C₂₆H₂₈FN₇O₄·1.8H₂O) C, H, N.

Methyl (2-Amino-1,3-oxazol-5-yl)acetate (19). Methyl 3-bromo-4-oxobutanoate (3 g, 15.4 mmol) in DMF (10 mL) was reacted with urea (1.25 g, 20.9 mmol) at 110 °C for 30 min. The solvent was evaporated and the residual oil was purified by silica gel chromatography, eluting with CH₂Cl₂:MeOH, NH₃ (7 N) (99:1 to 97.5:2.5) to give oxazole **19** as an oil (774 mg, 48%): ¹H NMR (DMSO-*d*₆) δ 3.64 (s, 3H), 3.66 (s, 2H), 6.48 (s, 1H), 6.49 (s, 2H); MS ESI⁺ *m/z* 157.3 (M + H)⁺.

Methyl (2-[[6-Methoxy-7-(3-morpholin-4-ylpropoxy)quinazolin-4-yl]amino]-1,3-oxazol-5-yl)acetate (23). Amidine **7** (500 mg, 1.4 mmol) in AcOH (1.2 mL) was heated with stirring with amino oxazole **19**⁴⁸ (237 mg, 1.52 mmol) at 135 °C under argon for 30 min. The solvent was evaporated, and the residual oil was purified by silica gel chromatography, eluting with CH₂Cl₂:MeOH, NH₃ (7 N) (99:1 to 97.5:2.5) to give ester **23** as a yellow solid (464 mg, 73%): ¹H NMR (DMSO-*d*₆, TFA) δ 2.28 (m, 2H), 3.15 (m, 2H), 3.36 (m, 2H), 3.55 (m, 2H), 3.67 (m, 2H), 3.7 (s, 3H), 3.97 (s, 2H), 4 (s, 3H), 4.02 (m, 2H), 4.3 (m, 2H), 7.34 (s, 1H), 7.42 (s, 1H), 7.77 (s, 1H), 8.89 (s, 1H); MS ESI⁺ *m/z* 458.6 (M + H)⁺.

N-(3-Fluorophenyl)-2-(2-[[6-methoxy-7-(3-morpholin-4-ylpropoxy)quinazolin-4-yl]amino]-1,3-oxazol-5-yl)acetamide (24). **Step 1.** Quinazolinone ester **23** (300 mg, 0.66 mmol) in solution in MeOH (7.5 mL) was saponified with NaOH (2 N, 7.5 mL) at 80 °C for 2 h. The MeOH was evaporated and the residue was treated with HCl (6 N, 6 mL). This was purified by chromatography over a Waters macroporous copolymer, Oasis, eluting successively with H₂O and H₂O:MeOH (1:1) to give (2-[[6-methoxy-7-(3-morpholin-4-ylpropoxy)quinazolin-4-yl]amino]-1,3-oxazol-5-yl)acetic acid as a yellow solid (273 mg, 94%): ¹H NMR (DMSO-*d*₆, TFA) δ 2.29 (m, 2H), 3.16 (m, 2H), 3.35 (m, 2H), 3.54 (m, 2H), 3.68 (m, 2H), 3.85 (s, 2H), 3.98 (s, 3H), 4.03 (m, 2H), 4.29 (m, 2H), 7.33 (s, 1H), 7.39 (s, 1H), 7.77 (s, 1H), 8.88 (s, 1H); MS ESI⁺ *m/z* 444.6 (M + H)⁺.

Step 2. (2-[[6-Methoxy-7-(3-morpholin-4-ylpropoxy)quinazolin-4-yl]amino]-1,3-oxazol-5-yl)acetic acid (130 mg, 0.29 mmol) in DMA (0.82 mL) was reacted with 3-fluoroaniline (32 μL, 0.35 mmol) in the presence of 2-hydroxypyridine *N*-oxide (39 mg, 0.35 mmol), EDCI (68 mg, 0.35 mmol), and DIEA (62 μL, 0.35 mmol) for 3 h at 50 °C. The DMA was evaporated and the residue purified by preparative LC-MS to give **24** as a yellow solid (108 mg, 69%): ¹H NMR (DMSO-*d*₆, TFA) δ 2.28 (m, 2H), 3.16 (m, 2H), 3.35 (t, 2H), 3.55 (d, 2H), 3.68 (t, 2H), 3.94 (s, 2H), 3.97 (s, 3H), 4.03 (m, 2H), 4.31 (m, 2H), 6.98 (m, 1H), 7.33 (s, 1H), 7.36 (m, 2H), 7.46 (s, 1H), 7.63 (m, 1H), 7.77 (s, 1H), 8.9 (s, 1H); MS ESI⁺ *m/z* 537 (M + H)⁺. Anal. (C₂₇H₂₉FN₆O₅·H₂O) C, H, N.

N-(4-Fluorophenyl)-2-[[6-methoxy-7-(3-morpholin-4-ylpropoxy)quinazolin-4-yl]amino]-1,3-thiazole-5-carboxamide (26). **Step 1.** Ester **25** (1.6 g, 3.4 mmol) in suspension in EtOH (32 mL) was reacted with NaOH (6 N, 6 mL) at 75 °C for 1 h. The cooled solution was acidified with HCl (6 N) to pH 4. The solid was filtered, washed with EtOH and then Et₂O, and dried to give 2-[[6-methoxy-7-(3-morpholin-4-ylpropoxy)quinazolin-4-yl]amino]-1,3-thiazole-5-carboxylic acid as a yellow solid (1.65 g, 86%): ¹H NMR (DMSO-*d*₆, TFA) δ 2.28 (m, 2H), 3.12 (t, 2H), 3.32 (t, 2H), 3.51 (d, 2H), 3.66 (t, 2H), 3.97 (s, 3H), 3.99 (d, 2H), 4.31 (t, 2H), 7.37 (s, 1H), 8.06 (s, 1H), 8.32 (s, 1H), 9.24 (s, 1H); MS ESI⁺ *m/z* 446 (M + H)⁺.

Step 2. 2-[[6-Methoxy-7-(3-morpholin-4-ylpropoxy)quinazolin-4-yl]amino]-1,3-thiazole-5-carboxylic acid (95 mg, 0.17 mmol) in DMF (1 mL) was reacted with 4-fluoroaniline (23 mg, 0.2 mmol) in the presence of *O*-(7-azabenzotriazol-1-yl)-*N,N,N',N'*-tetramethyluronium hexafluorophosphate (91 mg, 0.24 mmol) and DIEA (110 mg, 0.85 mmol) at 50 °C for 15 h. The reaction mixture was then treated with a solution of NaHCO₃ (1 mL) with stirring for

0.5 h and concentrated. The residue was washed with CH₂Cl₂:MeOH (1:1, 25 mL). Alumina was added to the organic phase, which was evaporated. Purification of the compound was carried out by chromatography over alumina eluting successively with CH₂Cl₂ and CH₂Cl₂:MeOH (95:5) to give **26** (58 mg, 64%): ¹H NMR (DMSO-*d*₆, TFA) δ 2.31 (m, 2H), 3.16 (t, 2H), 3.36 (t, 2H), 3.56 (d, 2H), 3.69 (t, 2H), 4.01 (s, 3H), 4.03 (d, 2H), 4.32 (t, 2H), 7.2 (t, 1H), 7.38 (s, 1H), 7.73 (m, 1H), 8.05 (s, 1H), 8.57 (s, 1H), 9.28 (s, 1H); MS ESI⁺ *m/z* 539 (M + H)⁺. Anal. (C₂₆H₂₇FN₆O₄·0.7H₂O) C, H, N, S.

N-(3-Fluorophenyl)-2-(2-[[6-methoxy-7-(3-morpholin-4-ylpropoxy)quinazolin-4-yl]amino]-1,3-thiazol-4-yl)acetamide (28). **Step 1.** Ester **27** (2 g, 4.1 mmol) was saponified as described for the preparation of **26**, step 1, to give (2-[[6-methoxy-7-(3-morpholin-4-ylpropoxy)quinazolin-4-yl]amino]-1,3-thiazol-4-yl)acetic acid as a yellow solid (1.99 g, 99%): ¹H NMR (DMSO-*d*₆, TFA) δ 2.31 (m, 2H), 3.16 (t, 2H), 3.35 (t, 2H), 3.56 (d, 2H), 3.71 (t, 2H), 3.79 (s, 2H), 4.0 (s, 3H), 4.03 (m, 2H), 4.31 (m, 2H), 7.25 (s, 1H), 7.34 (s, 1H), 8.01 (s, 1H), 9.13 (s, 1H); MS ESI⁺ *m/z* 460 (M + H)⁺.

Step 2. (2-[[6-Methoxy-7-(3-morpholin-4-ylpropoxy)quinazolin-4-yl]amino]-1,3-thiazol-4-yl)acetic acid (147 mg, 0.3 mmol) was condensed with 3-fluoroaniline (40 mg, 0.36 mmol) as described for the preparation of **26**, step 2, to give **28** (100 mg, 60%): ¹H NMR (DMSO-*d*₆, TFA) δ 2.3 (m, 2H), 3.16 (t, 2H), 3.36 (t, 2H), 3.56 (d, 2H), 3.69 (t, 2H), 3.91 (s, 2H), 3.99 (s, 3H), 4.04 (m, 2H), 4.31 (m, 2H), 6.9 (m, 1H), 7.29 (s, 1H), 7.33 (s, 1H), 7.37 (m, 2H), 7.64 (m, 1H), 8.01 (s, 1H), 9.13 (s, 1H); MS ESI⁺ *m/z* 553.3 (M + H)⁺. Anal. (C₂₇H₂₉FN₆O₄S) C, H, N.

N-(3-Fluorophenyl)-2-(2-[[6-methoxy-7-(3-morpholin-4-ylpropoxy)quinazolin-4-yl]amino]-1,3-thiazol-5-yl)acetamide (30). **Step 1.** Ester **29** (4.38 g, 8 mmol) was saponified as described for the preparation of **26**, step 1, to give (2-[[6-methoxy-7-(3-morpholin-4-ylpropoxy)quinazolin-4-yl]amino]-1,3-thiazol-5-yl)acetic acid (3.7 g, 100%): ¹H NMR (DMSO-*d*₆, TFA) δ 2.29 (m, 2H), 3.16 (t, 2H), 3.35 (t, 2H), 3.55 (d, 2H), 3.69 (t, 2H), 3.92 (s, 2H), 3.99 (s, 3H), 4.03 (m, 2H), 4.3 (m, 2H), 7.31 (s, 1H), 7.6 (s, 1H), 7.9 (s, 1H), 9.09 (s, 1H); MS ESI⁺ *m/z* 460 (M + H)⁺.

Step 2. (2-[[6-Methoxy-7-(3-morpholin-4-ylpropoxy)quinazolin-4-yl]amino]-1,3-thiazol-5-yl)acetic acid (77 mg, 0.17 mmol) was condensed with 3-fluoroaniline (23 mg, 0.21 mmol) as described for the preparation of **26**, step 2, to give **30** (35 mg, 40%): ¹H NMR (DMSO-*d*₆, TFA) δ 2.3 (m, 2H), 3.16 (t, 2H), 3.36 (t, 2H), 3.56 (d, 2H), 3.69 (t, 2H), 3.99 (s, 3H), 4.01 (s, 2H), 4.04 (m, 2H), 4.31 (m, 2H), 6.91 (m, 1H), 7.31 (s, 1H), 7.34 (m, 2H), 7.62 (m, 1H), 7.65 (s, 1H), 7.91 (s, 1H), 9.1 (s, 1H); MS ESI⁺ *m/z* 553.2 (M + H)⁺. Anal. (C₂₇H₂₉FN₆O₄S·4.1H₂O) C, H, N, S.

N'-(2-Cyano-5-hydroxy-4-methoxyphenyl)-N,N-dimethylimidofornamide (33). **8** (15.45 g, 50 mmol) in TFA (200 mL) was irradiated in a microwave oven at 75 °C for 45 min. The solvent was evaporated, and the residue was dissolved in CH₂Cl₂, washed with Na₂CO₃, and dried over MgSO₄. This was evaporated to give **33** as a pale yellow solid (10.26 g, 94%): ¹H NMR (DMSO-*d*₆, TFA) δ 3.24 (s, 3H), 3.34 (s, 3H), 3.87 (s, 3H), 7.02 (s, 1H), 7.49 (s, 1H), 8.56 (s, 1H); MS ESI⁺ *m/z* 220.5 (M + H)⁺.

N'-[5-(3-Chloropropoxy)-2-cyano-4-methoxyphenyl]-N,N-dimethylimidofornamide (34). **33** (439 mg, 2 mmol) in CH₃CN (5 mL) was reacted with 1-bromo-3-chloropropane (0.22 mL, 2.2 mmol) and Cs₂CO₃ (1.95 g, 5.98 mmol) at 85 °C for 0.5 h. The reaction mixture was evaporated, taken up in CH₂Cl₂:H₂O, extracted with CH₂Cl₂, dried over MgSO₄, and evaporated to give **34** as a pale yellow solid (450 mg, 76%): ¹H NMR (DMSO-*d*₆, TFA) δ 2.26 (t, 2H), 3.26 (s, 3H), 3.37 (s, 3H), 3.81 (t, 2H), 3.87 (s, 3H), 4.23 (t, 2H), 7.34 (s, 1H), 7.53 (s, 1H), 8.56 (s, 1H); MS ESI⁺ *m/z* 296.56 (M + H)⁺. Anal. (C₁₄H₁₈ClN₃O₂) C, H, Cl, N.

N'-[5-(2-Chloroethoxy)-2-cyano-4-methoxyphenyl]-N,N-dimethylimidofornamide (35). A mixture of **33** (12 g, 36 mmol), Cs₂CO₃ (52 g, 164 mmol), and 1-bromo-2-chloroethane (5 mL, 60 mmol) in CH₃CN (160 mL) was refluxed for 2 h. The reaction mixture was cooled, the solvent evaporated, and the residue was suspended in H₂O (300 mL). This was extracted with CH₂Cl₂ (2 ×

200 mL), and the organic solution was washed with brine (100 mL), dried over MgSO_4 , filtered, and evaporated. The residue was triturated with Et_2O , and the solid was collected and dried to yield **35** (8.2 g, 81% yield) as a white solid: $^1\text{H NMR}$ ($\text{DMSO}-d_6$) δ 2.98 (s, 3H), 3.02 (s, 3H), 3.78 (s, 3H), 3.95 (t, 2H), 4.3 (t, 2H), 6.75 (s, 1H), 7.08 (s, 1H), 7.9 (s, 1H); MS ESI^+ m/z 282 ($\text{M} + \text{H}$) $^+$.

2-(2-Amino-1,3-thiazol-5-yl)-N-(2,3-difluorophenyl)acetamide-7-(3-chloropropoxy)-6-methoxyquinazoline (38). A mixture **57** (2.31 g, 9.2 mmol) and **34** (2.71 g, 9.2 mmol) in AcOH (10 mL) was refluxed for 2 h. The mixture was cooled and the solid collected by filtration. The solid was rinsed with AcOH then Et_2O , dissolved in DMA (20 mL), and filtered. An aqueous Na_2CO_3 solution (50 mL) was added slowly to the filtrate and the solid collected by filtration, rinsed with H_2O , and dried to yield **38** (2.20 g, 46% yield): $^1\text{H NMR}$ ($\text{DMSO}-d_6$) δ 2.25 (m, 2H), 3.81 (t, 2H), 3.93 (s, 3H), 3.95 (s, 2H), 4.26 (t, 2H), 7.18 (m, 2H), 7.28 (s, 1H), 7.36 (s, 1H), 7.7 (m, 1H), 8.1 (s, 1H), 8.66 (s, 1H), 10.2 (br s, 1H), 11.96 (br s, 1H); MS ESI^+ m/z 520 ($\text{M} + \text{H}$) $^+$.

2-{2-[(7-{3-[Ethyl(2-hydroxyethyl)amino]propoxy}-6-methoxyquinazolin-4-yl)amino]-1,3-thiazol-5-yl]-N-(3-fluorophenyl)acetamide (41). A mixture of **37** (234 mg, 0.4 mmol) and 2-ethylaminoethanol (200 μL , 2.05 mmol) in DMA (2 mL) was heated at 80 $^\circ\text{C}$ under argon for 4 h. The reaction mixture was cooled, poured onto a silica gel column, and purified by chromatography eluting successively with CH_2Cl_2 and $\text{CH}_2\text{Cl}_2:\text{MeOH}$ (95:5), followed by $\text{CH}_2\text{Cl}_2:\text{MeOH}$, NH_3 (3 N) (92:8) to give **41** (82 mg, 41%): $^1\text{H NMR}$ ($\text{DMSO}-d_6$, TFA) δ 1.27 (t, 3H), 2.27 (m, 2H), 3.3 (m, 6H), 3.77 (t, 2H), 3.99 (s, 3H), 4.0 (s, 2H), 4.3 (t, 2H), 6.91 (t, 1H), 7.3 (s, 1H), 7.32 (d, 1H), 7.37 (q, 1H), 7.62 (d, 1H), 7.65 (s, 1H), 7.91 (s, 1H), 9.09 (s, 1H); MS ESI^+ m/z 555.6 ($\text{M} + \text{H}$) $^+$. Anal. ($\text{C}_{27}\text{H}_{31}\text{FN}_6\text{O}_4\text{S}\cdot 0.6\text{H}_2\text{O}$) C, H, N.

2-[(7-{3-[(2S)-2-(Hydroxymethyl)pyrrolidin-1-yl]propoxy}-6-methoxyquinazolin-4-yl)amino]-1,3-thiazol-5-yl]acetic Acid (50). A solution of **49** (1 g, 1.84 mmol) in DMA (7 mL) was reacted with (2S)-pyrrolidin-2-ylmethanol (908 μL , 9.2 mmol) at 90 $^\circ\text{C}$ for 3 h. The solvent was evaporated, and the crude reaction mixture was solubilized in EtOH and saponified with NaOH (6 N, 700 μL) at 80 $^\circ\text{C}$ for 3 h. The mixture was acidified with diluted HCl (2 N) to pH 3, evaporated, and dissolved in a mixture of $\text{MeOH}:\text{CH}_2\text{Cl}_2$ (4:6). DIEA (550 μL) was added to the mixture, which was filtered. The organic phase was evaporated and triturated with EtOH to yield **50** as a hygroscopic solid (300 mg, 60%): $^1\text{H NMR}$ ($\text{DMSO}-d_6$) δ 1.78 (m, 1H), 1.9 (m, 1H), 2.02 (m, 1H), 2.12 (m, 1H), 2.32 (m, 2H), 3.17 (m, 1H), 3.22 (m, 1H), 3.62 (m, 4H), 3.78 (m, 1H), 3.92 (s, 2H), 3.98 (s, 3H), 4.3 (t, 2H), 7.48 (s, 1H), 7.57 (s, 1H), 7.88 (s, 1H), 9.02 (s, 1H); MS ESI^+ m/z 474.6 ($\text{M} + \text{H}$) $^+$.

1-[3-({4-[(5-{2-[(3-Fluorophenyl)amino]-2-oxoethyl]-1,3-thiazol-2-yl)amino]-6-methoxyquinazolin-7-yl}oxy)propyl]piperidin-4-yl}methyl Dihydrogen Phosphate (54). **Step 1**. Compound **46** (5.41 g, 9.33 mmol) in DMA (50 mL) was treated with tetrazole (1.33 g, 19.0 mmol) and di-*tert*-butyldiethylphosphoramidite (5.8 g, 22 mmol) at 20 $^\circ\text{C}$, under an inert atmosphere, for 2 h. The reaction solution was cooled to -10 $^\circ\text{C}$ and a 30% hydrogen peroxide solution (2.3 mL, 20 mmol) was added dropwise over 5 min. After stirring for 2 h at 20 $^\circ\text{C}$, the reaction was quenched at -10 $^\circ\text{C}$ with a 0.5 N sodium thiosulfate solution. The mixture was extracted twice with EtOAc (300 mL), the organic solution dried and evaporated, and the resulting oil purified by chromatography on silica gel, eluting with $\text{MeOH}:\text{NH}_3:\text{CH}_2\text{Cl}_2$ (4:1:97). Evaporation of solvent and drying in vacuo yielded di-*tert*-butyl 1-(3-((4-((5-(2-(3-fluorophenyl)amino)-2-oxoethyl)-1,3-thiazol-2-yl)amino)-6-methoxyquinazolin-7-yl)oxy)propyl)piperidin-4-yl)methyl phosphate (6.66 g, 84% yield) as an orange foam: $^1\text{H NMR}$ ($\text{DMSO}-d_6$) δ 1.22 (m, 2H), 1.40 (s, 18H), 1.6 (m, 3H), 1.95 (m, 4H), 2.45 (m, 2H), 2.9 (m, 2H), 3.7 (m, 2H), 3.89 (s, 2H), 3.95 (s, 3H), 4.18 (m, 2H), 6.88 (m, 1H), 7.25 (s, 1H), 7.35 (m, 2H), 7.38 (s, 1H), 7.6 (m, 1H), 8.2 (s, 1H), 8.65 (s, 1H), 10.45 (s, 1H), 12 (br s, 1H); MS ESI^+ m/z 773 ($\text{M} + \text{H}$) $^+$.

Step 2. Di-*tert*-butyl 1-(3-((4-((5-(2-(3-fluorophenyl)amino)-2-oxoethyl)-1,3-thiazol-2-yl)amino)-6-methoxyquinazolin-7-yl)-

oxy)propyl)piperidin-4-yl)methyl phosphate (6.64 g, 8.6 mmol) in 1,4-dioxane (250 mL) was treated with HCl (4 N) in 1,4-dioxane (15 mL, 60 mmol) at 20 $^\circ\text{C}$ for 18 h. The solid product was collected by filtration and rinsed successively with 1,4-dioxane (100 mL), CH_3CN (100 mL), and then Et_2O (100 mL) and dried in vacuo to give compound **54** (6.73 g, 98% yield) as a yellow solid: $^1\text{H NMR}$ ($\text{DMSO}-d_6$) δ 1.6 (m, 2H), 1.9 (m, 3H), 2.35 (m, 2H), 2.97 (m, 2H), 3.2 (m, 2H), 3.55 (m, 2H), 3.7 (m, 2H), 3.95 (s, 3H), 4.03 (s, 2H), 4.3 (m, 2H), 6.9 (m, 1H), 7.38 (m, 2H), 7.45 (s, 1H), 7.6 (s, 1H), 7.65 (m, 1H), 7.85 (s, 1H), 9 (s, 1H), 10.6 (br s, 1H), 10.95 (s, 1H); MS ESI^+ m/z 661 ($\text{M} + \text{H}$) $^+$. Anal. ($\text{C}_{29}\text{H}_{34}\text{FN}_6\text{O}_7\text{PS}\cdot 0.75\text{HCl}\cdot 2.55\text{H}_2\text{O}$) C, H, N, Cl.

2-(2-Amino-1,3-thiazol-5-yl)-N-(3-fluorophenyl)acetamide (56). **Step 1**. Triphenyl methyl chloride (17.3 g, 62.2 mmol) was progressively added to a suspension of **55** (10 g, 58.1 mmol) in CH_2Cl_2 (150 mL) and Et_3N (8.91 mL, 63.9 mmol) at 0 $^\circ\text{C}$. The mixture was stirred for 2 h at room temperature. H_2O (100 mL) was added and the mixture was extracted with EtOAc . The organic phase was dried and concentrated, to give methyl [2-(tritylamino)-1,3-thiazol-5-yl]acetate an off-white solid (16.72 g, 69%): $^1\text{H NMR}$ ($\text{DMSO}-d_6$) δ 3.58 (s, 3H), 3.59 (s, 2H), 6.57 (s, 1H), 7.3 (m, 15H), 8.4 (s, 1H).

Step 2. Methyl [2-(tritylamino)-1,3-thiazol-5-yl]acetate (80.9 mg, 0.195 mol) in EtOH (600 mL) and THF (200 mL) was saponified with NaOH (1 N, 300 mL, 0.3 mol) at room temperature for 3 h. The solvent was partly evaporated and the pH of the solution adjusted to 2 with HCl (6 N) with cooling. The solid was filtered and washed with H_2O to give [2-(tritylamino)-1,3-thiazol-5-yl]acetic acid (70 g, 88%): $^1\text{H NMR}$ ($\text{DMSO}-d_6$) δ 3.48 (s, 2H), 6.57 (s, 1H), 7.3 (m, 15 H), 8.38 (s, 1H); MS ESI^+ m/z 400.5 ($\text{M} + \text{H}$) $^+$.

Step 3. [2-(Tritylamino)-1,3-thiazol-5-yl]acetic acid (15 g, 37.5 mmol) in DMF (110 mL) was reacted under argon with 3-fluoroaniline (4.69 mL, 48.7 mmol) in the presence of DIEA (8.47 mL, 48.7 mmol) and HATU (18.52 g, 48.7 mmol) at 50 $^\circ\text{C}$ for 18 h. The solvent was evaporated and the residue triturated with a mixture of $\text{CH}_2\text{Cl}_2:\text{AcOEt}$ (9:1) to give *N*-(3-fluorophenyl)-2-[2-(tritylamino)-1,3-thiazol-5-yl]acetamide (14.63 g, 79%): $^1\text{H NMR}$ ($\text{DMSO}-d_6$) δ 3.56 (s, 2H), 6.6 (s, 1H), 6.89 (t, 1H), 7.28 (m, 17 H), 7.56 (d, 1H), 8.41 (s, 1H); MS ESI^- m/z 492.5 ($\text{M} - \text{H}$) $^-$.

Step 4. *N*-(3-Fluorophenyl)-2-[2-(tritylamino)-1,3-thiazol-5-yl]acetamide (14.69 g, 29.7 mmol) was stirred for 1 h in a mixture of TFA (100 mL) and H_2O (10 mL). H_2O (150 mL) was added to the reaction mixture, and the precipitated solid was recovered and washed with H_2O . The solid was purified by silica gel chromatography, eluting with $\text{CH}_2\text{Cl}_2:\text{MeOH}$ (90:10) to give **56** (6.21 g, 83%): $^1\text{H NMR}$ ($\text{DMSO}-d_6$) δ 3.65 (s, 2H), 6.76 (m, 3H), 6.9 (t, 1H), 7.29 (d, 1H), 7.36 (q, 1H), 7.59 (d, 1H); MS ESI^+ m/z 252.5 ($\text{M} + \text{H}$) $^+$.

5-(3-Fluorophenoxy)-1,3-thiazol-2-amine (59).⁴⁹ 3-Fluorophenol (3.6 mL, 39.75 mmol) dissolved in CH_3CN (80 mL) was slowly added over 50 min to a solution of **58** (5.37 g, 30 mmol) in CH_3CN (30 mL) in the presence of Cs_2CO_3 (14.7 g, 45 mmol) at 70 $^\circ\text{C}$. The mixture was heated for 1.5 h, cooled, and filtered; the organic phase was concentrated; and the residue purified by flash silica gel chromatography. Eluting successively with CH_2Cl_2 and $\text{CH}_2\text{Cl}_2:\text{MeOH}$ (8:2) yielded **59** (2.01 g, 32%): $^1\text{H NMR}$ ($\text{DMSO}-d_6$) δ 6.78 (s, 1H), 6.94 (m, 5H), 7.42 (m, 1H); MS ESI^+ m/z 211.4 ($\text{M} + \text{H}$) $^+$.

3-Fluoro-N-({2-[(7-{3-[4-(hydroxymethyl)piperidin-1-yl]propoxy}-6-methoxyquinazolin-4-yl)amino]-1,3-thiazol-5-yl}methyl)benzamide (66). **Step 1**. $\text{NH}_2\text{OH}\cdot\text{HCl}$ (7.16 g, 103 mmol), followed by pyridine (8.3 mL, 103 mmol), was added to a solution of **63**⁵¹ (18 g, 79 mmol) in EtOH (150 mL). The mixture was heated under argon for 2 h. EtOH was evaporated, the residue was triturated with H_2O , and a white solid was collected. This solid was washed with H_2O and dried to give *tert*-butyl {5-[(*E*)-(hydroxyimino)methyl]-1,3-thiazol-2-yl}carbamate (19.4 g, 100%): $^1\text{H NMR}$ ($\text{DMSO}-d_6$) δ 1.49 (s, 9H), 7.74 (s, 1H), 7.75 (s, 1H); MS ESI^- m/z 242.4 ($\text{M} - \text{H}$) $^-$.

Step 2. Zinc powder (925 mg, 15 mmol) was added to a solution of *tert*-butyl {5-[(*E*)-(hydroxyimino)methyl]-1,3-thiazol-2-yl}-

carbamate (729 mg, 3 mmol) in EtOAc (8 mL) and AcOH (8 mL), and the resulting mixture was heated at 45 °C for 1.5 h. This reaction mixture was cooled, filtered, concentrated, and the residue was purified by flash silica gel chromatography eluting successively with CH₂Cl₂:MeOH (9:1) and CH₂Cl₂:MeOH, NH₃ (3 N) (9:1) to give *tert*-butyl [5-(aminomethyl)-1,3-thiazol-2-yl]carbamate (440 mg, 64%): ¹H NMR (DMSO-*d*₆) δ 1.49 (s, 9H), 3.81 (s, 2H), 7.12 (s, 1H).

Step 3. 3-Fluorobenzoyl chloride (2.33 g, 14.7 mmol) in solution in CH₂Cl₂ (15 mL) was slowly added to a solution of *tert*-butyl [5-(aminomethyl)-1,3-thiazol-2-yl]carbamate (3.2 g, 14 mmol) and Et₃N (1.56 g, 15.4 mmol) in CH₂Cl₂ (35 mL) at 0 °C under argon. The mixture was stirred for 40 min at 0 °C and evaporated and the residue triturated with H₂O. A white solid was recovered, washed with H₂O, and dried to give *tert*-butyl (5-[(3-fluorobenzoyl)amino]methyl)-1,3-thiazol-2-yl]carbamate (5.1 g, 100%): ¹H NMR (DMSO-*d*₆) δ 1.48 (s, 9H), 4.54 (d, 2H), 7.26 (s, 1H), 7.43 (m, 1H), 7.54 (m, 1H), 7.67 (m, 1H), 7.74 (d, 1H), 9.2 (t, 1H); MS ESI⁺ *m/z* 352.5 (M + H)⁺.

Step 4. *tert*-Butyl (5-[(3-fluorobenzoyl)amino]methyl)-1,3-thiazol-2-yl]carbamate (4.8 g, 13.7 mmol) was dissolved in a mixture of CH₂Cl₂ (20 mL) and TFA (30 mL) and stirred at room temperature for 3 h. The mixture was evaporated, the residue was dissolved in EtOAc and washed with a saturated solution of NaHCO₃, and the resultant precipitate was recovered. The aqueous phase was extracted with AcOEt, and the organic phases were combined and dried to give **64** (3.12 g, 91%): ¹H NMR (DMSO-*d*₆) δ 4.41 (d, 2H), 6.79 (s, 2H), 6.83 (s, 1H), 7.4 (m, 1H), 7.54 (m, 1H), 7.64 (m, 1H), 7.71 (d, 2H), 9.06 (t, 1H); MS ESI⁺ *m/z* 252.4 (M + H)⁺.

Step 5. An analogous reaction to that described for the preparation of **37** but starting with **64** (2.8 g, 11.1 mmol) and **34** (3.14 g, 10.6 mmol) and heating at 135 °C for 1 h yielded *N*-[2-[[7-(3-chloropropoxy)-6-methoxyquinazolin-4-yl]amino]-1,3-thiazol-5-yl]methyl]-3-fluorobenzamide (4.11 g, 77%): ¹H NMR (DMSO-*d*₆) δ 2.27 (m, 2H), 3.83 (t, 2H), 3.97 (s, 3H), 4.29 (t, 2H), 4.64 (d, 2H), 7.28 (s, 1H), 7.41 (m, 1H), 7.45 (s, 1H), 7.55 (m, 1H), 7.7 (d, 1H), 7.77 (d, 1H), 8.12 (s, 1H), 8.67 (s, 1H), 9.25 (t, 1H); MS ESI⁺ *m/z* 502.4 (M + H)⁺.

Step 6. An analogous reaction to that described for the preparation of **41** but starting with piperidin-4-ylmethanol (92 mg, 0.81 mmol) and *N*-[2-[[7-(3-chloropropoxy)-6-methoxyquinazolin-4-yl]amino]-1,3-thiazol-5-yl]methyl]-3-fluorobenzamide (115 mg, 0.23 mmol) yielded **66** (93 mg, 69%): ¹H NMR (DMSO-*d*₆, TFA) δ 1.42 (m, 2H), 1.65 (m, 1H), 1.87 (m, 2H), 2.3 (m, 2H), 2.97 (t, 2H), 3.27 (t, 2H), 3.31 (d, 2H), 3.6 (d, 2H), 3.98 (s, 3H), 4.29 (t, 2H), 4.63 (s, 2H), 7.29 (s, 1H), 7.4 (m, 1H), 7.55 (m, 1H), 7.7 (m, 1H), 7.71 (s, 1H), 7.76 (d, 1H), 7.9 (s, 1H), 9.09 (s, 1H); MS ESI⁺ *m/z* 581.5 (M + H)⁺. Anal. (C₂₉H₃₃FN₆O₄S·0.8H₂O) C, H, N, S.

3-Fluoro-*N*-[2-[[7-(3-[4-(hydroxymethyl)piperidin-1-yl]propoxy)-6-methoxyquinazolin-4-yl]amino]-1,3-thiazol-5-yl]methyl]-benzenesulfonamide (67). **Step 1.** 3-Fluorobenzoyl chloride (4.09 g, 21 mmol) in solution in pyridine (15 mL) was slowly added to a solution of *tert*-butyl [5-(aminomethyl)-1,3-thiazol-2-yl]carbamate (3.21 g, 14 mmol) in pyridine (50 mL) at 0 °C under argon. The mixture was stirred at room temperature for 3 h, the solvent was evaporated, and the residue was dissolved in CH₂Cl₂ and washed with a saturated solution of NaHCO₃. The aqueous phase was extracted with CH₂Cl₂, the organic phases were combined and concentrated, and the residue was purified by silica gel chromatography eluting with CH₂Cl₂:MeOH (95:5 to 90:10) to give *tert*-butyl [5-[(3-fluorophenyl)sulfonyl]amino]methyl)-1,3-thiazol-2-yl]carbamate (4.8 g, 78%): ¹H NMR (DMSO-*d*₆) δ 1.49 (s, 9H), 4.18 (s, 2H), 7.09 (s, 1H), 7.51 (m, 1H), 7.55 (m, 1H), 7.63 (m, 2H); MS ESI⁺ *m/z* 388.4 (M + H)⁺.

Step 2. An analogous reaction to that described in the synthesis of **66**, step 4, but starting with *tert*-butyl [5-[(3-fluorophenyl)sulfonyl]amino]methyl)-1,3-thiazol-2-yl]carbamate (4.7 g, 12.1 mmol) yielded **65** (3.6 g, 100%): ¹H NMR (DMSO-*d*₆) δ 4.03 (s, 2H), 6.68 (s, 1H), 6.85 (s, 2H), 7.52 (m, 2H), 7.64 (m, 2H), 8.2 (br s, 1H); MS ESI⁺ *m/z* 288.4 (M + H)⁺.

Step 3. An analogous reaction to that described in the synthesis of **66**, step 5, but starting with **65** (3.31 g, 11.5 mmol) and **34** (3.25 g, 11 mmol) yielded *N*-[2-[[7-(3-chloropropoxy)-6-methoxyquinazolin-4-yl]amino]-1,3-thiazol-5-yl]methyl]-3-fluorobenzesulfonamide (4.95 g, 84%): ¹H NMR (DMSO-*d*₆) δ 2.28 (m, 2H), 3.84 (t, 2H), 3.97 (s, 3H), 4.3 (m, 4H), 7.3 (s, 2H), 7.52 (m, 1H), 7.64 (m, 2H), 7.68 (s, 1H), 8.11 (s, 1H), 8.4 (br s, 1H), 8.68 (s, 1H); MS ESI⁺ *m/z* 538.3 (M + H)⁺.

Step 4. An analogous reaction to that described in the synthesis of **66**, step 6, but starting with *N*-[2-[[7-(3-chloropropoxy)-6-methoxyquinazolin-4-yl]amino]-1,3-thiazol-5-yl]methyl]-3-fluorobenzesulfonamide (130 mg, 0.23 mmol) and piperidine-4-ylmethanol (92 mg, 0.8 mmol) yielded **67** (103 mg, 73%): ¹H NMR (DMSO-*d*₆, TFA) δ 1.42 (m, 2H), 1.64 (m, 1H), 1.88 (m, 2H), 2.3 (m, 2H), 2.99 (t, 2H), 3.28 (t, 2H), 3.32 (d, 2H), 3.6 (d, 2H), 3.98 (s, 3H), 4.27 (s, 2H), 4.29 (t, 2H), 7.32 (s, 1H), 7.52 (m, 1H), 7.57 (s, 1H), 7.66 (m, 2H), 7.72 (s, 1H), 7.92 (s, 1H), 9.12 (s, 1H); MS ESI⁺ *m/z* 617.5 (M + H)⁺. Anal. (C₂₈H₃₃FN₆O₅S₂·0.6H₂O) C, H, N.

Biological Evaluation. IC₅₀ values reported are average figures of at least two independent measurements.

Aurora B Kinase Inhibition. Recombinant Enzyme Assay. Recombinant Aurora B bound to its activating partner protein INCENP (0.24 mg/mL) with an activity of 22 units/mL was purchased from Dundee University. The enzyme complex was diluted 1:100 in enzyme dilution buffer (50 μL of 1 M Tris pH 7.5, 25 μL of 1 M KCl, 1.2 μL of 1 M DTT, and 1.924 mL of distilled water) and 20 μL of the diluted enzyme was added to each assay well of a 96-well plate. Compounds were tested in duplicate at eight concentrations (10–0.0045 μM final concentration) as well as a reference compound, blank wells, and control wells. A 20-μL portion of the reaction mixture (62.5 μL of 1 M Tris-HCl pH 7.5, 31.8 μL of 1 M KCl, 6.25 μL of 1 M NaF, 1.5 μL of 1 M DTT, 15.62 μL of 1 M MnCl₂, 218.75 μL of 1 mM ATP, 31.25 μL of 500 μM biotin tetra-LRRWSLG peptide, 2.07 mL of distilled water, and 25 μCi of [γ-³³P]ATP Redivue for a total volume of 2500 μL) was added to all wells. The plates were gently mixed and incubated for 1 h at room temperature. The reaction was stopped by adding 100 μL of 20% v/v phosphoric acid to all wells. The peptide was captured on a P30 filtermat (Wallac 1205–406) using a Tomtec micro-cell-harvester. Filter mats were washed with phosphate buffer and dried in an oven set at 70 °C until dry. Filter mats were bagged (sample bags Wallac 1205–411), and 16 mL of BetaScint (JIT CBET001) was added. Filter mats were rolled to ensure all positions are soaked with scintillant. Bags were sealed and counted on a Wallac Beta Counter. IC₅₀ values were calculated using ORIGIN Scientific Graphing Analyses.

Aurora A Inhibition. Recombinant Enzyme Assay. Recombinant A was produced at AstraZeneca (full length human wild-type AuroraA purified from Sf9 cells infected with a recombinant baculovirus expressing Aurora A). The enzyme complex was diluted 1:200 in enzyme dilution buffer (50 μL of 1 M Tris pH 7.5, 25 μL of 1 M KCl, 1.2 μL of 1 M DTT, and 1.924 mL of distilled water). A 20-μL portion of the diluted enzyme was added to each well. Compounds were tested in duplicate, with each plate containing five compounds at eight concentrations (10–0.003 μM final concentration) as well as a reference compound, blank wells, and control wells. A 20-μL aliquot of reaction mixture (25 μL of 1 M Tris-HCl pH 7.5, 12.75 μL 1 M KCl, 2.5 μL of 1 M NaF, 0.6 μL of 1 M DTT, 6.25 μL of 1 M MnCl₂, 25 μL of 1 mM ATP, 15 μL of 500 μM biotin tetra-LRRWSLG peptide, 912.25 μL of distilled water, and 10 μCi of [γ-³³P]ATP Redivue) was added to all wells using an Eppendorf repeater. The plates were gently mixed and incubated for 1 h at room temperature. The reaction was stopped by adding 100 μL of 20% v/v phosphoric acid to all wells, and the samples were processed as for the Aurora B assay described above.

In Vitro Measure of Cellular Levels of Phosphohistone (Serine 10) H3. SW620 cells (10⁴ per well) were plated in 100 μL of DMEM media (containing 10% fetal calf serum and 1% glutamine) in costar 96-well plates and left overnight at 37 °C and 5% CO₂ to adhere.

These cells were then dosed with compound diluted in media (50 μL is added to each well to give 0.00015–1 μM concentrations of compound).

After 24 h of treatment with compound, the cells were fixed by addition of 100 μL of 3.7% formaldehyde to each well for 30 min at room temperature. The fixative was decanted and the wells washed once with 100 μL of phosphate buffer saline (PBS). The PBS was subsequently aspirated, and the cells were permeabilized by addition of 100 μL of PBS 0.5% Triton X-100 for 5 min. The wells were then washed with 100 μL of PBS prior to the addition of 50 μL of primary antibody (rabbit anti-phosphohistone H3 06-750 purchased from Upstate Biotechnology), diluted 1:500 in PBS 1% BSA and 0.5% Tween for 1 h. The wells were then washed twice with PBS. In an unlit area, 50 μL of secondary antibody (Alexa Fluor 488 goat anti-rabbit IgG cat. no. 11008 molecular probes), diluted 1:10 000 in PBS plus 1% bovine serum albumin, 0.5% Tween was added for 1 h at room temperature. The wells were then washed with 200 μL of PBS. Finally, 100 μL of PBS was added to each well, and the plates were sealed ready to analyze. Analysis was carried out using a Cellomics Arrayscan II instrument and the Cellomics Arrayscan Target Activation algorithm to measure cellular levels of phosphohistone H3. Results are reported as IC₅₀ values for inhibition of phosphorylation of histone H3 and are averages of two independent measurements.

Selectivity Profile in a Panel of Kinases. Assays Description.

A panel of 4 serine-threonine kinase assays (CDK2, JNK1A, P38A, PKA) were established by utilizing generic buffers, reagents, and filter capture technology. In brief, the enzyme reaction was performed in 96-well plates (MATRIX ScreenMates cat #4917). The reaction was initiated by the addition of ATP/substrate mix to the enzyme in the presence or absence of test compounds. The concentration of cold/hot ATP (NEN Life Science Products "EasyTides" NEG 602H (10 mCi/mL) is $\leq K_m$ for the specific enzyme. The reaction was performed at room temperature and terminated by the addition of 50% v/v orthophosphoric acid following a predefined incubation period specific for each enzyme. The addition of 70% w/v TCA was incorporated to help in the precipitation of proteins. The terminated incubation mixture was rapidly harvested utilizing the TomTec harvester 9600 and the precipitate was captured using Packard UniFilter-96, GF/C 96 well filter plates. The plates were washed with 1.5% v/v orthophosphoric acid followed by absolute alcohol, scintillation cocktail (Packard Bioscience code 6013621) was added to all wells, and activity was recorded using a Packard TopCount scintillation counter.

A panel of nine tyrosine kinase assays [CSK, EGFR, FAK, FGFR, IGFR, JAK3, KDR, MEK (dual kinase), SRC] was established utilizing generic buffers, reagents, and traditional ELISA technology. In brief, the enzyme reaction was performed in 384-well plates (MATRIX ScreenMates #4311). The plates were coated with pEAY (Sigma P3899) or enzyme-specific substrate for a minimum of 24 h and washed prior to use using phosphate buffered saline + Tween 20 (PBST) and 50 mmol Hepes. The reaction was initiated by the addition of enzyme to ATP/cofactor mix in the presence or absence of test compounds. The concentration of ATP was $\leq K_m$ for the specific enzyme. The reaction was performed at room temperature and terminated by the addition of 0.5 M EDTA following a predefined incubation period specific for each enzyme. The plates were washed with PBST and 4G10-HRP anti-phosphotyrosine antibody (UBI 16–105) or an assay-specific antibody added to all wells. Following a further incubation, the plates were washed with PBST, and either TMB (Sigma T2885) or a secondary antibody was applied. The TMB reaction is terminated by the addition of 2 M H₂SO₄, the same signal detection procedure is applied to those enzymes requiring two antibodies, although the wash buffer is PBS/A. The optical density is measured on the TECAN Ultra plate reader at 450 nm.

In Vivo Studies. Swiss *nu/nu* (nude) mice were bred and housed in negative-pressure isolators (PFI Systems Ltd, Oxon, UK) at Alderley Park, UK. Experiments were conducted on 8–10-week-old male mice in full accordance with the UK Home Office Animal (Scientific Procedures) Act 1986. Human tumor xenografts were

established by injecting 1×10^6 SW620 tumor cells [contained within 100 μL of 50:50 Matrigel (Fred Baker, Liverpool, UK) and serum-free media], subcutaneously on the dorsal flank of mice. Tumors were measured biweekly with callipers and tumor volumes were calculated as described previously.⁵² Pharmacodynamic studies were conducted when tumors reached a mean size of approximately 0.2 cm³. Compounds were prepared in Tris buffer pH 9 and administered as a continuous infusion for up to 48 h via subcutaneously implanted Alzet osmotic minipumps (Model 2001D, Fisher Scientific, UK) in accordance with manufacturer's instructions. Groups of mice (four mice per group) were sacrificed at intervals of up to 48 h after compound administration, and plasma samples were snap-frozen in liquid nitrogen while tumors were processed to paraffin wax blocks in a standard manner. Tissue sections were cut (3–4 μm thick) and stained with an antibody directed against Ser10 phospho-histone H3 (Upstate Biotechnology, Dundee, UK), followed by an Envision one-step HRP-labeled polymer method (DakoCytomation, Ely, Cambridgeshire). Labeling was detected with diaminobenzidine substrate solution (DakoCytomation, Ely, Cambridgeshire), and sections were counter stained with Carazzi's hematoxylin. Analysis of phospho-histone H3 stained cells in tumors sections was performed on a Zeiss KS400 (version 3) image analysis system (Imaging Associates Ltd, Bicester, Oxford) linked to a Leica DMRB microscope. Group means were compared by using Student's one-tailed, unpaired *t* test. Probability (*P*) values less than 0.05 were interpreted as significant.

Molecular Modeling and Quantum Chemical Calculations.

The molecular models were built using SYBYL molecular modeling software with the standard bond distances and angles (version 6.9.1).⁵³ The ligand geometries were optimized by energy minimization using the parameter set included in the AMPAC (version 6.55A) suite of programs,⁵⁴ with the AM1 Hamiltonian. The thiazole and oxazole models were minimized using ab initio molecular orbital calculations at the RHF/3-21G* level.³⁴ The energy of the investigated conformers was subsequently calculated at the 6-31G* level. For the imidazole model, the geometries were optimized at the 6-31G* level.

Acknowledgment. The authors thank Dr. Kevin Foote for helpful comments and suggestions, Dr. Richard Pauptit for supplying a ligand complexed structure of Aurora A, Dr. Dave Timms for modeling support, Mr. Colin Bath for supplying the kinase panel assays experimental procedures, Mr. Christian Delvare and Dr. Delphine Dorison Duval for their spectrometric and analytical support, and Mr. Jacques Pelleter, Mr. Patrice Koza, and Mr. Dominique Boucherot for helpful large-scale and robotic synthesis support.

Supporting Information Available: Experimental details and data for compounds **3**, **5**, **8**, **16**, **25**, **27**, **29**, **31**, **32**, **36**, **37**, **40**, **44–49**, **51–53**, **57**, and **60–62**, including results from elemental analyses for all target compounds of this study. This material is available free of charge via the Internet at <http://pubs.acs.org>.

References

- (1) Bischoff, J. R.; Plowman, G. D. The Aurora/Ipl1p kinase family: regulators of chromosome segregation and cytokinesis. *Trends Cell Biol.* **1999**, *9*, 454–459.
- (2) Bischoff, J. R.; Anderson, L.; Zhu, Y.; Mossie, K.; Ng, L.; Souza, B.; Schryver, B.; Flanagan, P.; Clairvoyant, F.; Ginther, C.; Chan, C. S. M.; Novotny, M.; Salomon, D. J.; Plowman, G. D. A homologue of Drosophila Aurora kinase is oncogenic and amplified in colorectal cancers. *EMBO J.* **1998**, *17*, 3052–3065.
- (3) Zhou, H.; Kuang, J.; Zhong, L.; Kuo, W. L.; Gray, J. W.; Sahin, A.; Brinkley, B. R.; Sen, S. Tumour amplified kinase STK15/BTAK induces centrosome amplification, aneuploidy and transformation. *Nat. Genet.* **1998**, *20*, 189–193.
- (4) Carmana, M.; Earnshaw, W. C. The cellular geography of Aurora kinases. *Nat. Rev. Mol. Cell Biol.* **2003**, *4*, 842–854.
- (5) Murata-Hori, M.; Wang, Y. The kinase activity of Aurora B is required for kinetochore-microtubule interactions in mitosis. *Curr. Biol.* **2002**, *12*, 894–899.

- (6) Adams, R. R.; Maiato, H.; Earnshaw, W. C.; Carmena, M. Essential role of *Drosophila* inner centromere protein (INCENP) and Aurora B in histone H3 phosphorylation, metaphase chromosome alignment, kinetochore disjunction, and chromosome segregation. *J. Cell. Biol.* **2001**, *153*, 865–880.
- (7) Biggins, S.; Murray, A. W. The budding yeast protein kinase Ipl1/Aurora allows the absence of tension to activate the spindle checkpoint. *Genes Dev.* **2001**, *15*, 3118–3129.
- (8) Dietchfield, C.; Johnson, V. L.; Tighe, A.; Ellston, R.; Haworth, C.; Johnson, T.; Mortlock, A.; Keen, N.; Taylor, S. S. Aurora B couples chromosome alignment with anaphase by targeting BubR1, Mad2, and Cenp-E to kinetochores. *J. Cell. Biol.* **2003**, *161*, 267–280.
- (9) Bishop, J. D.; Schumacher, J. M. Phosphorylation of the carboxyl terminus of inner centromere protein (INCENP) by Aurora B kinase stimulates Aurora B kinase activity. *J. Biol. Chem.* **2002**, *277*, 27577–27580.
- (10) Tanaka, T. U.; Rachidi, N.; Janke, C.; Pereira, G.; Glova, M.; Schiebel, E.; Stark, M. J. R.; Nasmyth, K. Evidence that Ipl1-Sli15 (Aurora kinase-INCENP) complex promotes bi-orientation by altering kinetochore-spindle pole connections. *Cell* **2002**, *108*, 317–329.
- (11) Shimoda, S. L.; Solomon, F. Integrating functions at the kinetochore. *Cell* **2002**, *109*, 9–12.
- (12) Wheatley, S. P.; Carvalho, A.; Vagnarelli, P.; Earnshaw, W. C. INCENP is required for proper targeting of Survivin to the centromeres and the anaphase spindle during mitosis. *Curr. Biol.* **2001**, *11*, 886–890.
- (13) Bolton, M. A.; Lan, W.; Powers, S. E.; McClelland, M. L.; Kuang, J.; Stukenberg, P. T. Aurora B Kinase exists in a complex with Survivin and INCENP and its kinase activity is stimulated by Survivin binding and phosphorylation. *Mol. Biol. Cell* **2002**, *13*, 3064–3077.
- (14) Adams, R. R.; Carmena, M.; Earnshaw, W. C. Chromosomal passengers and the (Aurora) ABCs of mitosis. *Trends Cell Biol.* **2001**, *11*, 49–54.
- (15) Chen, J.; Jin, S.; Tahir, S. K.; Zhang, H.; Liu, X.; Sarthy, A. V.; McGonigal, T. P.; Liu, Z.; Rosenberg, S. H.; Ng, S. C. Survivin enhances Aurora-B kinase activity and localizes Aurora-B in human cells. *J. Biol. Chem.* **2003**, *278*, 486.
- (16) Meraldi, P.; Honda, R.; Nigg, E. A. Aurora-A overexpression reveals tetraploidation as a major route to centrosome amplification in p53^{-/-} cells. *EMBO J.* **2002**, *21*, 483–492.
- (17) Anaud, S.; Penrhyn-Lowe, S.; Venkiteraman, A. R. Aurora-A amplification overrides the mitotic spindle assembly checkpoint, inducing resistance to taxol. *Cancer Cell* **2003**, *3*, 51–62.
- (18) Jallepalli, P. V.; Lengauer, C. Chromosome segregation and cancer: Cutting through the mystery. *Nat. Rev. Cancer* **2001**, *1*, 109–117.
- (19) Hsu, J. Y.; Sun, Z. W.; Li, X.; Reuben, M.; Tatchell, K.; Bishop, D. K.; Grushcow, J. M.; Brame, C. J.; Caldwell, J. A.; Hunt, D. F.; Lin, R.; Smith, M. M.; Allis, C. D. Mitotic phosphorylation of histone H3 is governed by Ipl1/Aurora kinase and Glc 7/PP1 phosphatase in budding yeasts and nematodes. *Cell* **2000**, *102*, 279–291.
- (20) Giet, R.; Glover, D. M. *Drosophila* Aurora B kinase is required for histone H3 phosphorylation and condensin recruitment during chromosome condensation and to organize the central spindle during cytokinesis. *J. Cell. Biol.* **2001**, *152*, 669–682.
- (21) Crosio, C.; Fimia, G. M.; Loury, R.; Kimura, M.; Okano, Y.; Zhou, H.; Sen, S.; Allis, C. D.; Sassone-Corsi, P. Mitotic phosphorylation of histone H3: Spatio-temporal regulation by mammalian Aurora kinases. *Mol. Cell. Biol.* **2002**, *22*, 874–885.
- (22) Giet, R.; Prigent, C. Aurora/Ipl1p-related kinases, a new family of mitotic serine-threonine kinases. *J. Cell Sci.* **1999**, *112*, 3591–3601.
- (23) Tatsuka, M.; Katayama, H.; Ota, T.; Tanaka, T.; Odashima, S.; Suzuki, F.; Terada, Y. Multinuclearity and increased ploidy caused by overexpression of the Aurora-and Ipl1-like midbody-associated protein mitotic kinase in human cancer cells. *Cancer Res.* **1998**, *58*, 4811–4816.
- (24) Harrington, E. A.; Bebbington, D.; Moore, J.; Rasmussen, R. K.; Ajose-Adeogun, A. O.; Nakayama, T.; Graham, J. A.; Demur, C.; Hercend, T.; Diu-Hercend, A.; Su, M.; Golec, J. M. C.; Miller, K. M. VX-680, a potent and selective small-molecule inhibitor of the Aurora kinases, suppresses tumour growth in vivo. *Nat. Med.* **2004**, *10*, 262–267.
- (25) Hauf, S.; Cole, R. W.; LaTerra, S.; Zimmer, C.; Schnapp, G.; Walter, R.; Heckel, A.; Van Meel, J.; Rieder, C. L.; Peters, J.-M. The small molecule Hesperadin reveals a role for Aurora B in connecting kinetochore-microtubule attachment and in maintaining the spindle assembly checkpoint. *J. Cell Biol.* **2003**, *161*, 281–294.
- (26) Rewcastle, G. W.; Denny, W. A.; Bridges, A. J.; Zhou, H.; Cody, D. R.; McMichael, A.; Fry, D. W. Tyrosine kinase inhibitors. Synthesis and structure–activity relationships for 4-((phenylmethyl)-amino)- and 4-(phenylamino)quinazolines as potent adenosine 5'-triphosphate binding site inhibitors of the tyrosine kinase domain of the epidermal growth factor receptor. *J. Med. Chem.* **1995**, *38*, 3482–3487.
- (27) Tsou, H.-R.; Mamuya, N.; Johnson, B. D.; Reich, M. F.; Gruber, B. C.; Ye, F.; Nilakanatan, R.; Shen, R.; Discifani, C.; DeBlanc, R.; Davis, R.; Koehn, F. E.; Greenberger, L. M.; Wang, Y.-F.; Wissner, A. 6-substituted-4-(3-bromophenylamino)quinazolines as putative irreversible inhibitors of epidermal growth factor receptor (EGFR) and human epidermal growth factor receptor (HER-2) tyrosine kinases with enhanced antitumour activity. *J. Med. Chem.* **2001**, *44*, 2719–2734.
- (28) Traxler, P.; Bold, G.; Frei, J.; Lang, M.; Lydon, N.; Mett, H.; Buchdunger, E.; Meyer, T.; Mueller, M.; Furet, P. Use of a pharmacophore model for the design of EGF-R tyrosine kinase inhibitors: 4-(Phenylamino)pyrazolo[3,4-d]pyrimidines. *J. Med. Chem.* **1997**, *40*, 3601–3616.
- (29) Mortlock, A. A.; Jung, F. H. Preparation of substituted quinazoline derivatives and their use as inhibitors of Aurora-2 kinase. WO 2002000649 A1 20020103. CAN 136:85826.
- (30) Jung, F. H.; Pasquet, G. R. Preparation of substituted quinazoline derivatives as inhibitors of Aurora kinases. WO 2003055491 A1 20030710. CAN 139:101142.
- (31) Mortlock, A. A.; Keen, N. J.; Jung, F. H.; Heron, N. M.; Foote, K. M.; Wilkinson, R.; Green, S. Progress in the Development of Selective Inhibitors of Aurora kinases. *Curr. Top. Med. Chem.* **2005**, *5*, 199–213.
- (32) Heron, N. M.; Anderson, M.; Blowers, D. P.; Breed, J.; Eden, J. M.; Green, S.; Hill, G. B.; Johnson, T.; Jung, F. H.; McMiken, H. H. J.; Mortlock, A. A.; Pannifer, A. D.; Pauptit, R. A.; Pink, J.; Roberts, N. J.; Rowsell, S. SAR and Inhibitor Complex Structure Determination of a Novel Class of Potent and Specific Aurora Kinase Inhibitors. *Bioorg. Med. Chem. Lett.* In press.
- (33) Frisch, M. J.; Trucks, G. W.; Schlegel, H. B.; Scuseria, G. E.; Robb, M. A.; Cheeseman, J. R.; Zakrzewski, V. G.; Montgomery, J. A., Jr.; Stratmann, R. E.; Burant, J. C.; Dapprich, S.; Millam, J. M.; Daniels, A. D.; Kudin, K. N.; Strain, M. C.; Farkas, O.; Tomasi, J.; Barone, V.; Cossi, M.; Cammi, R.; Mennucci, B.; Pomelli, C.; Adamo, C.; Clifford, S.; Ochterski, J.; Petersson, G. A.; Ayala, P. Y.; Cui, Q.; Morokuma, K.; Malick, D. K.; Rabuck, A. D.; Raghavachari, K.; Foresman, J. B.; Cioslowski, J.; Ortiz, J. V.; Stefanov, B. B.; Liu, G.; Liashenko, A.; Piskorz, P.; Komaromi, I.; Gomperts, R.; Martin, R. L.; Fox, D. J.; Keith, T.; Al-Laham, M. A.; Peng, C. Y.; Nanayakkara, A.; Gonzalez, C.; Challacombe, M.; Gill, P. M. W.; Johnson, B. G.; Chen, W.; Wong, M. W.; Andres, J. L.; Head-Gordon, M.; Replogle, E. S.; Pople, J. A. *Gaussian 98*, revision A. 11. 3; Gaussian, Inc.: Pittsburgh, PA, 2002.
- (34) Pierce, A. C.; ter Haar, E.; Binch, H. M.; Kay, D. P.; Patel, S. R.; Li, P. CH...O and CH...N Hydrogen Bonds in Ligand Design: A Novel Quinazolin-4-ylthiazol-2-ylamine Protein Kinase Inhibitor. *J. Med. Chem.* **2005**, *48*, 1278–81.
- (35) Bayliss, R.; Sardon, T.; Vernos, I.; Conti, E. Structural basis of Aurora-A activation by TPX2 at the mitotic spindle. *Mol. Cell.* **2003**, *12*, 851–862.
- (36) Nowakowski, J.; Cronin, C. N.; McRee, D. E.; Knuth, M. W.; Nelson, C. G.; Pavletich, N. P.; Rogers, J.; Sang, B. C.; Scheibe, D. N.; Swanson, R. V.; Thompson, D. A. Structures of the cancer-related aurora-A, FAK, and EphA2 protein kinases from nanovolume crystallography. *Structure* **2002**, *10*, 1659–1667.
- (37) Cheatham, G. M. T.; Knegtel, R. M. A.; Coll, J. T.; Renwick, S. B.; Swenson, L.; Weber, P.; Lippke, J. A.; Weisberg, D. A. Crystal structure of aurora-2, an oncogenic serine/threonine kinase. *J. Biol. Chem.* **2002**, *277*, 42419–42422.
- (38) Nagar, B.; Bornmann, W. G.; Pellicena, P.; Schindler, T.; Veach, D. R.; Miller, W. T.; Clarkson, B.; Kuriyan, J. Crystal structures of the kinase domain of c-Abl in complex with the small molecule inhibitors PD173955 and imatinib (STI-571). *Cancer Res.* **2002**, *62*, 4236–4243.
- (39) Pargellis, C.; Tong, L.; Churchill, L.; Cirillo, P. F.; Gilmore, T.; Graham, A. G.; Grob, P. M.; Hickey, E. R.; Moss, N.; Pav, S.; Regan, J. Inhibition of P38 MAP kinase by utilizing a novel allosteric binding site. *Nat. Struct. Biol.* **2002**, *9*, 268–272.
- (40) Wan, P. T. C.; Garnett, M. J.; Roe, S. M.; Lee, S.; Niculescu-Duvaz, D.; Good, V. M.; Cancer Genome Project; Jones, C. M.; Marshall, C. J.; Springer, C. J.; Barford, D.; Marais, R. Mechanism of Activation of the RAF-ERK Signaling Pathway by Oncogenic Mutations of B-RAF. *Cell* **2004**, *116* (6), 855–67.

- (41) Sessa, F.; Mapelli, M.; Ciferri, C.; Tarricone, C.; Araces, L. B.; Schneider, T. R.; Stukenberg, P. T.; Musacchio, A. Mechanism of Aurora B Activation by INCENP and Inhibition by Hesperadin. *Cell*. **2005**, *18* (3), 379–91.
- (42) Hennequin, L. F.; Thomas, A. P.; Johnstone, C.; Stokes, E. S. E.; Plé, P. A.; Lohmann, J. J. M.; Ogilvie, D. J.; Dukes, M.; Wedge, S. R.; Curven, J. O.; Kendrew, J.; Lambert-van der Brempt, C. Design and structure–activity relationship of a new class of potent VEGF receptor tyrosine kinase inhibitors. *J. Med. Chem.* **1999**, *42*, 5369–5389.
- (43) Hennequin, L. F.; Stokes, E. S. E.; Thomas, A. P.; Johnstone, C.; Plé, P. A.; Ogilvie, D. J.; Dukes, M.; Wedge, S. R.; Kendrew, J.; Curven, J. O. Novel 4-anilinoquinazolines with C7 basic side chains: Design and structure activity relationship of a series of potent, orally active, VEGF receptor tyrosine kinase inhibitors. *J. Med. Chem.* **2002**, *45*, 1300–1312.
- (44) Pandey, A.; Volkots, D. L.; Seroogy, J. M.; Rose, J. W.; Yu, J. C.; Lambing, J. L.; Hutchaleelaka, A.; Hollenbach, S. J.; Abe, K.; Giese, N. A.; Scarborough, R. M. Identification of orally active, potent and selective 4-piperazinylquinazolines as antagonists of the platelet-derived growth factor receptor tyrosine kinase family. *J. Med. Chem.* **2002**, *45*, 3772–3793.
- (45) Smaill, J. B.; Rewcastle, G. W.; Loo, J. A.; Greis, K. D.; Chan, O. H.; Reyner, E. L.; Lipka, E.; Showalter, H. D. H.; Vincent, P. W.; Elliot, W. L.; Denny, W. A. Tyrosine kinase inhibitors. 17. Irreversible inhibitors of epidermal growth factor receptor. 4-(Phenylamino)-quinazoline- and 4-(phenylamino)pyrido[3,2-*d*]pyrimidine-6-acrylamides bearing additional solubilizing functions. *J. Med. Chem.* **2000**, *43*, 1380–1397.
- (46) Erlenmeyer, H.; Herzfeld, L.; Prijs, B. Zur synthese von 2-amino-thiazolderivaten. *Helv. Chem. Acta* **1955**, *38*, 1291–1294.
- (47) Molina, P.; Conesa, C.; Velasco, M. D. Iminophosphorane-mediated synthesis of 2-aminoimidazole derivatives. *Synthesis* **1996**, 1459–1462.
- (48) Gompper, R.; Christmann, O. Studies in the azole series. *Chem. Ber.* **1959**, *92*, 1944–1949.
- (49) El-Kerdawy, M. M.; El-Emam, A. A.; El-Subbagh, H. I.; Abushanab, E. Synthesis of substituted 4*H*-thiazolo[4,5-*b*][1]benzothioopyran-4-ones as possible schistosomicidal agents. *Monatsch. Chem.* **1989**, *120*, 991–995.
- (50) Mahajanshetti, C. S.; Basanagoudar, L. D. A facile nucleophilic displacement of bromine in 2-amino-4-methyl-5-bromothiazole by a thiophenoxide anion. *Can. J. Chem.* **1967**, *45*, 1807–1810.
- (51) Harada, H.; Watanuki, S.; Takuwa, T.; Kawaguchi, K.; Okazaki, T.; Hirano, Y.; Saitoh, C. Preparation of dicyanopyridine derivatives as high-conductance calcium-sensitive potassium channel openers. WO 20026237 A1 20020124. CAN 136:118474.
- (52) Wedge, S. R.; Ogilvie, D. J.; Dukes, M.; Kendrew, J.; Curven, J. O.; Hennequin, L. F.; Thomas, A. P.; Stokes, E. S. E.; Curry, B.; Richmond, G. H. P.; Wadsworth, P. F. ZD4190: An orally active inhibitor of vascular endothelial growth factor signaling with broad-spectrum antitumor efficacy. *Cancer Res.* **2000**, *60*, 970–975.
- (53) SYBYL 6.9.1; Tripos Inc., St. Louis, MO.
- (54) AMPAC, version 6.55 A.; Semichem Inc.: Kansas City, MO, 1999.
- (55) Fancelli, D.; Berta, D.; Bindi, S.; Cameron, A.; Cappella, O.; Carpinelli, P.; Catana, C.; Forte, B.; Giordano, P.; Giorgini, M. L.; Mantegani, S.; Marsiglio, A.; Meroni, M.; Moll, J.; Pittalà, V.; Roletto, F.; Severino, D.; Soncini, C.; Storici, P.; Tonani, R.; Varasi, M.; Vulpetti, A.; Vianello, P. Potent and Selective Aurora Inhibitors Identified by the Expansion of a Novel Scaffold for Protein Kinase Inhibition. *J. Med. Chem.* **2005**, *48*, 3080–3084.
- (56) McWeeny, R. *Methods of Molecular Quantum Mechanics*, 2nd ed.; Elsevier Academic Press: New York, 1992.

JM050786H